

# NASA TECHNICAL MEMORANDUM

**NASA TM X-71610**

**NASA TM X-71610**

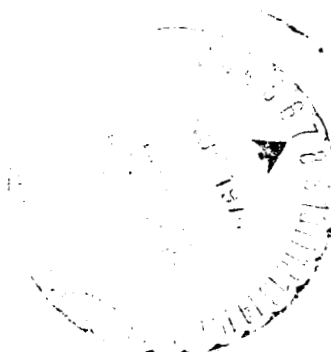
(NASA-TM-X-7161C) EFFECT OF INLET  
INGESTION OF A WING TIP VORTEX ON  
TURBOJET STALL MARGIN (NASA) 57 p HC  
\$3.75 CSCI 21E

N74-35201

G3/28      Unclass  
51095

EFFECT OF INLET INGESTION OF A WING TIP VORTEX  
ON TURBOJET STALL MARGIN

by Glenn A. Mitchell  
Lewis Research Center  
Cleveland, Ohio  
September 1974



**M M M M M M M M M M M M M M M M M M**

# ABSTRACT

A two-dimensional inlet and J85-GE-13 turbojet engine were placed in a Mach 0.4 stream so as to ingest the tip vortex of a forward mounted wing. Results show that ingestion of a wing tip vortex by a turbojet engine can cause a large reduction in engine stall margin. The loss in stall compressor pressure ratio was primarily dependent on vortex location and rotational direction and not on total-pressure variations across the compressor face.

E-8091

# EFFECT OF INLET INGESTION OF A WING TIP VORTEX ON TURBOJET STALL MARGIN

by Glenn A. Mitchell

Lewis Research Center

## SUMMARY

A two-dimensional inlet and J85-GE-13 turbojet engine were placed in a Mach 0.4 stream in the Lewis 10- by 10-Foot Supersonic Wind Tunnel so as to ingest the tip vortex of a forward mounted wing. The vortex was ingested at various vertical locations across the inlet entrance. Wing angle variations were utilized to produce vortices of maximum strength that rotated either with or opposite to the engine rotation.

Results show that ingestion of a wing tip vortex by a turbojet engine can cause a large reduction in engine stall margin. Stall occurred at a compressor pressure ratio that was as much as 33 percent (along a line of constant corrected speed) closer to the nominal normal operating line than the undistorted inflow stall line. Vortex location at the compressor face and vortex rotational direction had a significant effect on stall compressor pressure ratio. Vortex induced stall pressure ratios did not correlate with total-pressure variations across the compressor face.

## INTRODUCTION

Some aircraft require the use of forward mounted stub wings for stability and control purposes. At large angles of attack, such a wing would generate a strong tip vortex. With propulsion systems mounted on or close to the fuselage, it is probable that certain combinations of airplane pitch and yaw would cause the vortex to trail aft into the engine air inlet. The effects of such a vortex ingestion on engine operating characteristics are unknown but may be degrading enough to cause engine stall.

A study of these phenomena was conducted in the Lewis 10- by 10-Foot Supersonic Wind Tunnel with the test section operating at a subsonic speed of Mach 0.4. Reynolds number was  $7.5 \times 10^6$  per meter. A wing was mounted in the test section forward of a two-dimensional inlet-engine combination so that the tip vortex trailed aft into the inlet and impinged on the J85-GE-13 engine compressor face. A preliminary study using the inlet with a coldpipe (ref. 1) found that the strongest vortex was created by the wing at 11 degrees angle of attack. The maximum tangential velocity of the vortex, just prior to its entering the inlet, was 57 percent of the local stream velocity. Tangential velocities at the simulated compressor face were as high as 25 percent of the local stream velocity. This report presents the effect of this vortex ingestion on the stall limits of the J85-GE-13 turbojet engine.

U.S. Customary Units were used in the design of the test model and for the recording of experimental data. These units were converted to the International System of Units for presentation in this report.

## SYMBOLS

c	wing tip chord, cm
H	vertical distance from cowl lip to ramp edge, cm
h	vertical distance from cowl lip to initial position where vortex impinged on cowl lip, cm
N	engine speed, rpm
N <sup>*</sup>	rated engine speed, 16 500 rpm
$(N/N^*\sqrt{\theta}) \times 100$	percent corrected engine speed
P	total pressure, N/m <sup>2</sup>
T	total temperature, K
W	engine air flow, kg/sec
W <sub>corr</sub>	engine corrected air flow, $W\sqrt{\theta}/\delta$ , kg/sec
x	streamwise (axial) distance aft from wing tip trailing edge, cm
$\delta$	local corrected total pressure, $P/101\ 325\ \text{N/m}^2$
$\theta$	local corrected total temperature, $T/288.2\ \text{K}$

## Subscripts:

iv	ingested vortex
u	undistorted
2	compressor face
3	compressor exit

## Superscript:

—	average
---	---------



## APPARATUS AND PROCEDURE

## Inlet

The inlet used in this investigation was a two-dimensional, external-compression type designed for operation at a Mach number of 2.2. The inlet was attached to a nacelle 0.635 meter in diameter in which a J85-GE-13 turbojet engine or a cold-pipe choked-exit plug assembly could be installed. For this study the J85-GE-13 engine was used. The inlet, with the cold-pipe assembly as used in reference 1, is shown in figure 1 mounted in the tunnel test section. The inlet height (ramp edge to cowl lip) was 0.408 meter and the ramp width was 0.369 meter.

The inlet geometry was varied by movable ramps. The first ramp was a fixed one, having an angle of 3 degrees with the inlet at zero degrees angle of attack. The second and third ramps were variable and together with the first ramp accomplished external compression during supersonic operation. The fourth ramp was a backward facing ramp which initiated internal flow diffusion. For this test the inlet throat area was opened to a maximum by setting the ramps as flat as possible. The resulting second and third ramp angles of  $5\frac{1}{3}$  and  $7\frac{2}{3}$  degrees measured relative to the inlet at zero degrees angle of attack are shown in figure 1. A bleed slot between the third and fourth ramp was available for boundary layer control. All bleed and bypass systems were closed for this test.

Three basic variations exist between the inlet configuration shown in the figure and the configuration used during this test. The vortex generators shown in figure 1 on the ramp and side walls were not present for this test. Also the side fairings and cowl lip were not sharp as shown. The leading edge of the side fairings were blunted with a radius of 0.42 centimeter. The cowl lip was 0.76 centimeter thick and blunted with a 3 to 1 ellipse.

## Engine

The J85-GE-13 engine consists of an eight-stage axial-flow compressor coupled directly to a two-stage turbine. It incorporates controlled compressor interstage bleed and variable inlet guide vanes, a through-flow annular combustor, and an afterburner (not used in this test) with a variable area primary exhaust nozzle. Engine installation is shown in figure 2.

At sea-level conditions and military power operation, the eight-stage compressor develops an overall static pressure ratio of 7.0. The pressure ratio per stage averages out to 1.275.

The compressor interstage bleed valves (located after the third, fourth, and fifth compressor stages) are mechanically linked to the variable inlet guide vanes so that when the bleed valves are fully open, the guide vanes are fully closed. The inlet guide vanes are linked together

and scheduled by the main fuel control as a function of corrected speed. This provides the normal interstage bleed schedule. For stall attempts during this test and for all comparison data presented herein, the guide vanes were computer controlled on a nonstandard schedule providing the maximum allowable bleed closure for safe engine operation as dictated by compressor blade vibration limits. This procedure was required to obtain the maximum assurance of engine stall at corrected speeds below 94 percent of rated speed.

Compressor stalls were initiated by closing the exhaust nozzle. In order to lower turbine temperatures during this procedure, the first stage turbine nozzle was replaced by a unit approximately 14 percent smaller in area. This rematched the turbine to the compressor at a lower than normal turbine inlet temperature.

At engine speeds below 90 percent of rated speed, manual closure of the standard exhaust nozzle resulted in minimum nozzle areas that were too large to cause compressor stall. To obtain smaller nozzle areas (and higher compressor pressure ratios), six airflow blockage plates were installed inside the nozzle leaves.

Steady state operation of the J85-GE-13 engine, while coupled to an axisymmetric mixed-compression inlet is reported in reference 2. Reference 3 reports transient interactions between the engine and the same inlet.

### Wing

Details of the wing are shown in figure 3. The wing had a slight aft sweep of the leading edge and a forward sweep of the trailing edge. Also, the wing was symmetrical with parallel upper and lower surfaces over much of the chord. The leading edge was a 4.52 to 1 ellipse and the trailing edge was formed by a 25 degree included angle and faired into the straight sides of the wing.

The wing was mounted in the tunnel test section forward of the inlet and extended vertically down from a circular inset in the tunnel ceiling (fig. 4). Wing angle of attack was varied by rotating the circular inset. The inlet location aft of the wing (fig. 5) placed the ramp edge 8.2 wing-tip chord lengths downstream of the wing-tip trailing edge. A typical vortex path from the wing to the inlet is shown in figures 5 and 6. This path was produced by the wing at +11 degrees angle of attack (ref. 1). The inlet is shown at zero degree angle of attack. The inlet was placed at various vertical locations relative to the vortex trailing aft from the wing by pitching the inlet to various angles of attack. Maximum angle-of-attack variation during the test was from zero to -7 degrees. As indicated in figure 5, positive angle of attack was opposite to the normal convention. This was because the inlet was mounted upside down in the tunnel.

### Test Procedure

With a given wing angle of attack, a series of stall attempts were made at each selected engine corrected airflow. Each stall attempt of the series occurred with the vortex entering the inlet at a different vertical location between the cowl lip and the inlet ramp edge. Prior to each series, a vertical location reference point was obtained by pitching the inlet and using the tunnel schlieren system to visually impinge the center of the trailing vortex on the cowl lip.

All stall attempts were initiated at the lowest compressor pressure ratio available at the selected engine corrected airflow. The initial condition was achieved by controlling the throttle to set the selected corrected airflow while keeping the exhaust nozzle open. The stall point was approached by closing the nozzle to increase the compressor pressure ratio while manually biasing the throttle to keep a constant compressor face static- to total-pressure ratio (i.e., a constant corrected airflow).

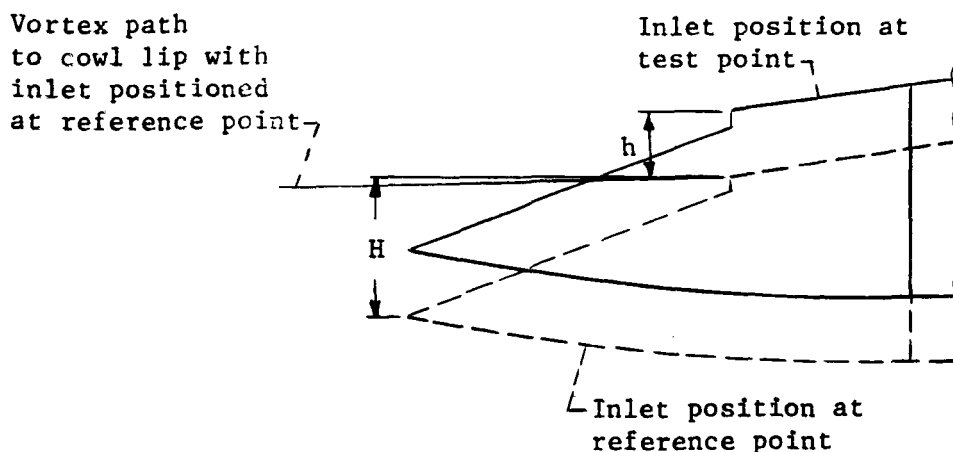
Stalls were attempted at a constant corrected airflow rather than a constant engine speed in order to keep the entering vortex at a constant position as stall was approached. Reference 1 reports that the vortex path in the vicinity of the inlet was affected by the airflow streamlines approaching the inlet in a manner such that the vertical position of the vortex at the inlet entrance varied with inlet mass flow ratio, i.e., corrected airflow.

Steady state data points presented later in this report as the points of stall were obtained at a compressor pressure ratio as close to stall as possible without stall occurring during the data scan. For most of these points stall occurred after the data scan; for others the pressure ratio was within 0.04 of the pressure ratio where stall occurred. When no stall occurred, data points were taken at the highest pressure ratio obtainable without exceeding the turbine discharge temperature limit of 1017 K.

## RESULTS AND DISCUSSION

Figure 10 presents the compressor performance that was obtained with the ingested vortex rotating counter to the engine rotation. Data were taken, up to the pressure ratio at stall or the turbine temperature limit, at three nominal corrected airflows and are plotted on a compressor map which was obtained with undistorted inflow to the engine in a connected pipe test (ref. 4). Both the current data and the data of reference 4 were obtained with the same inlet guide vane and compressor interstage bleed schedules. The maximum corrected airflow was limited to 18 kilograms per second because higher airflows would have required the engine to exceed its rated mechanical speed when operated near the undistorted stall line.

The data in figure 10 are shown for various values of the ingested vortex vertical position parameter. This parameter gives the approximate vertical position of the vortex relative to the inlet (see sketch).



The numerator of the parameter (h) is the vertical distance of the cowl lip from the previously mentioned reference point (vortex on lip) as calculated by geometric relations and the inlet change in pitch angle from the reference point. The denominator (H) is simply the vertical distance from the cowl lip to the inlet ramp edge. The ratio (h/H) would then determine the vertical distance of the entering vortex from the cowl lip in relation to the inlet height; but only if the vortex path was unaffected by inlet vertical position. This was probably not true at the axial location of the cowl lip when the vortex was near the ramp and affected by the flow turning induced by the ramp angles. This could not be visually observed because of the inlet side fairings.

As shown by figure 10, large reductions in stall margin from that obtained with undistorted inflow were observed when the ingested vortex rotated counter to the engine rotation. The largest stall margin losses were obtained when the ingested vortex vertical position parameter was near 0.5 (fig. 10(e)). And for a nominal engine corrected airflow of 16.5, nearly half of the undistorted inflow stall margin (vertical distance from normal operating line to stall line) was lost due to the entering vortex.

Figure 11 is a replot of the data of figure 10. Compressor pressure ratios are plotted against corrected engine speed. A comparison of figures 10 and 11 illustrates the fact that the stall pressure ratios caused by the entering vortex are nearer to the pressure ratios of the undistorted inflow stall line at a constant corrected speed than they are at a constant corrected airflow. Thus the method chosen for presenting the data can significantly affect the computed loss in stall pressure ratio.

Figures 12 and 13 present the stall data obtained with the ingested vortex rotating in the same direction as the engine rotation. Both the compressor maps (fig. 12) and the compressor pressure ratio against corrected engine speed plots (fig. 13) show (when compared to figs. 10 and 11) that the vortex rotational direction had a significant effect on the stall pressure ratio. For example, compare figure 10(e) to figure 12(e). At 16.5 kilograms per second nominal corrected airflow the compressor stalled at a pressure ratio of 5.63 when the vortex rotated counter to the engine and at a pressure ratio of 6.19 when the vortex rotated in the same direction as the engine.

The data that are presented in figures 10 to 13 are lacking somewhat in completeness due to the fact that, at the higher and lower corrected airflows, the turbine temperature limit prevented engine operation up to the pressure ratios of the undistorted inflow stall line. At the higher corrected airflow, stall sometimes occurred below the temperature limit adding to the data completeness; but at the lower corrected airflow stalls were never obtained.

It was decided that the most pertinent method of presenting the loss in stall compressor pressure ratio was at a constant corrected engine speed because the engine cannot significantly change speed during the few milli-

seconds spanning the occurrence of stall. Stall data are summarized in figure 14. The loss in stall compressor pressure ratio caused by the ingested vortex was computed from figures 11 and 13 at a constant corrected engine speed and plotted in a nondimensional form against the ingested vortex vertical position parameter. Data are also shown in figure 14 for the cases where the turbine temperature limit was reached before stall occurred.

The large losses in stall compressor pressure ratio caused by the ingested vortex are illustrated well in figure 14. The maximum loss in stall compressor pressure ratio caused by the ingested vortex rotating counter to the engine rotation was larger than the maximum loss in stall pressure ratio caused by the vortex rotating with the engine. When the vortex rotated counter to the engine, the maximum nondimensional loss in stall pressure ratio was 0.058 (fig. 14(a)); whereas when the vortex rotated with the engine rotation the maximum nondimensional loss in stall pressure ratio was 0.026 (fig. 14(b)). A better perspective of the significance of these numbers is gained by the realization that the 0.058 nondimensional loss in stall pressure ratio represents a stall pressure ratio that was 33 percent nearer to the nominal normal operating line (along a line of constant corrected speed) than the undistorted inflow stall line. The 0.026 nondimensional loss in stall pressure ratio caused by the vortex rotating with the engine was 15 percent nearer to the nominal normal operating line than the undistorted inflow stall line.

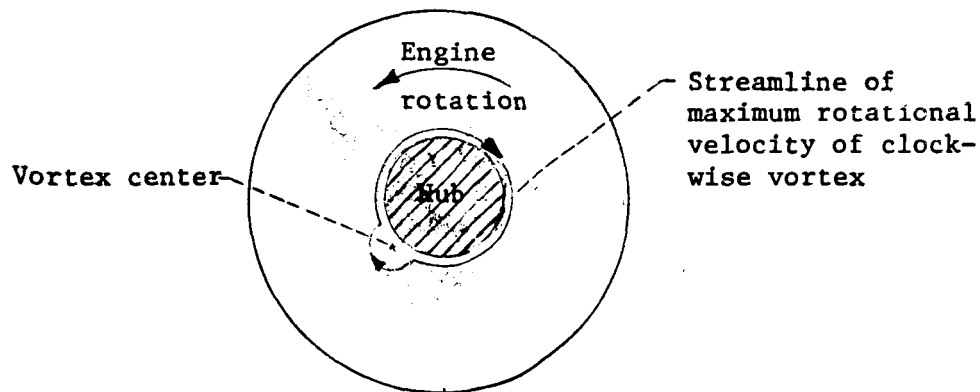
Figure 15 presents a correlation of the ingested vortex vertical position parameter with the measured radial position of the vortex at the compressor face. Although the radial positions of the vortex that are presented in the figure are for a specific vortex rotational direction and engine corrected airflow, they are typical in that the radial positions do not vary substantially with engine conditions or vortex rotational direction. The radial positions of the vortex were obtained from analysis of compressor-face total-pressure profiles that are not presented herein. The vortex core contained a lower total pressure which was detected by the total-pressure probes and traced from probe to probe as the vortex position varied across the inlet entrance.

It is clear from figures 14 and 15 that, when the ingested vortex was rotating counter to the engine rotation, the maximum loss in stall compressor pressure ratio occurred at the higher corrected airflows when the vortex was located near the engine hub. When the vortex rotated with the engine rotation the maximum loss in stall pressure ratio occurred again at the higher corrected airflows but the vortex was approximately midway between the hub and tip on the cowl side of the duct. These data not only show an effect of vortex rotational direction on the stall pressure ratio but also that the vortex position at the compressor face greatly influenced the stall pressure ratio. However, the dissimilar position effects of the clockwise and counterclockwise vortices strongly suggest that the effect of vortex position alone cannot be interpreted without also considering the influence of the rotational direction of the vortex and its effects on the engine.

At the lower engine corrected airflow where no stalls were obtained the turbine temperature limit line in figure 14 indicates that the non-dimensional loss in stall pressure ratio could not have exceeded about 0.03; roughly half of the maximum loss in stall pressure ratio incurred at the higher corrected airflows with the vortex rotating counter to the engine (fig. 14(a)); but about the same as the maximum loss in stall pressure ratio incurred at the higher corrected airflows with the vortex rotating with the engine (fig. 14(b)). Because of the different stall results between the higher and lower engine corrected airflows (fig. 14(a)) it seems that the vortex induced stall characteristics of the engine changed considerably at lower airflows.

The compressor-face total-pressure profiles generated during this test revealed that at each ingested vortex position the profiles obtained with clockwise and counterclockwise rotating vortices were, with small variations, mirror images of each other, especially those at the same engine corrected airflow. This fact, coupled with the above dissimilar effects of vortex rotational direction on stall, make it clear that no interpretation of the total-pressure variations across the compressor face could correlate them with vortex induced stall compressor pressure ratios.

The vortex stall effects reported herein must then be dependent on the rotational properties of the vortex. The maximum rotational velocity of the vortex at the compressor face was as large as 25 percent of the local stream velocity (ref. 1), with a diameter of about 4.5 centimeters; less than half the compressor hub diameter. The probable streamline of the vortex maximum rotational velocity as it expanded and wrapped around the engine hub when the vortex was located near the hub is shown in the sketch.



The resulting large rotational velocities near the hub and totally around its circumference explain the large loss in stall pressure ratio that occurred when the vortex was near the hub and rotating counter to the

engine. With such a condition fluid rotational velocities would appear to the compressor blades as a continual large increase in angle of attack near the hub and thereby increase the likelihood of stall. A contributing factor to this increased stall potential may be due to a characteristic of the engine reported in reference 4; when tip, mid-span, and hub radial distortion patterns were imposed upon the compressor, the hub region was found to be the most sensitive to distortion.

## SUMMARY OF RESULTS

A two-dimensional inlet-engine combination was placed in a Mach 0.4 stream in the Lewis 10- by 10-Foot Supersonic Wind Tunnel so as to ingest the tip vortex of a wing mounted at a forward location in the test section. Inlet angle-of-attack variation was used to cause vortex ingestion to occur at selected vertical locations across the inlet entrance. Wing angle of attack was selected to produce the maximum vortex strength, and positive and negative angles were utilized to generate vortices that rotated with and opposite to the direction of turbojet engine rotation. The effect of these variables on the stall margin of the J85-GE-13 turbojet engine was determined at three corrected airflows with the following results.

1. Ingestion of a wing tip vortex by a turbojet engine can cause a large reduction in engine stall margin.
2. Vortex location at the compressor face and vortex rotational direction had a significant effect on the compressor pressure ratio at which stall occurred.
3. Vortex induced stall compressor pressure ratios did not correlate with total-pressure variations across the compressor face.
4. With the vortex rotating opposite to the engine rotation and located near the compressor hub, the engine stalled at a compressor pressure ratio that was closer to the normal operating line than the undistorted inflow pressure ratio by as much as 33 percent along a line of constant corrected speed.
5. With the vortex and engine rotating in the same direction, the maximum loss in stall pressure ratio was smaller and occurred when the vortex was located on the cowl side of the duct about midway between the hub and tip. The stall pressure ratio was as much as 15 percent closer to the normal operating line than the undistorted inflow stall line.



## REFERENCES

1. Mitchell, Glenn A.: Preliminary Investigation of Inlet Ingestion of a Wing Tip vortex. NASA TM X-68225, 1973
2. Coltrin, Robert E.; and Choby, David A.: Steady-State Interactions from Mach 1.98 to 2.58 between a Turbojet Engine and an Axisymmetric Inlet with 60-Percent Internal Area Contraction. NASA TM X-1780, 1969.
3. Choby, David A.; Burstadt, Paul L.; and Calogeras, James E.: Unstart and Stall Interactions between a Turbojet Engine and an Axisymmetric Inlet with 60-Percent Internal Area Contraction. NASA TM X-2192, 1971.
4. Calogeras, James E.; Johnsen, Roy L.; and Burstadt, Paul L.: Effect of Screen-Induced Total-Pressure Distortion on Axial-Flow Compressor Stability. NASA TM X-3017, 1974.

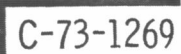


Figure 1. - Inlet model installed in 10- by 10-Foot Supersonic Wind Tunnel.

REPRODUCIBILITY OF THE  
ORIGINAL PAGE IS POOR

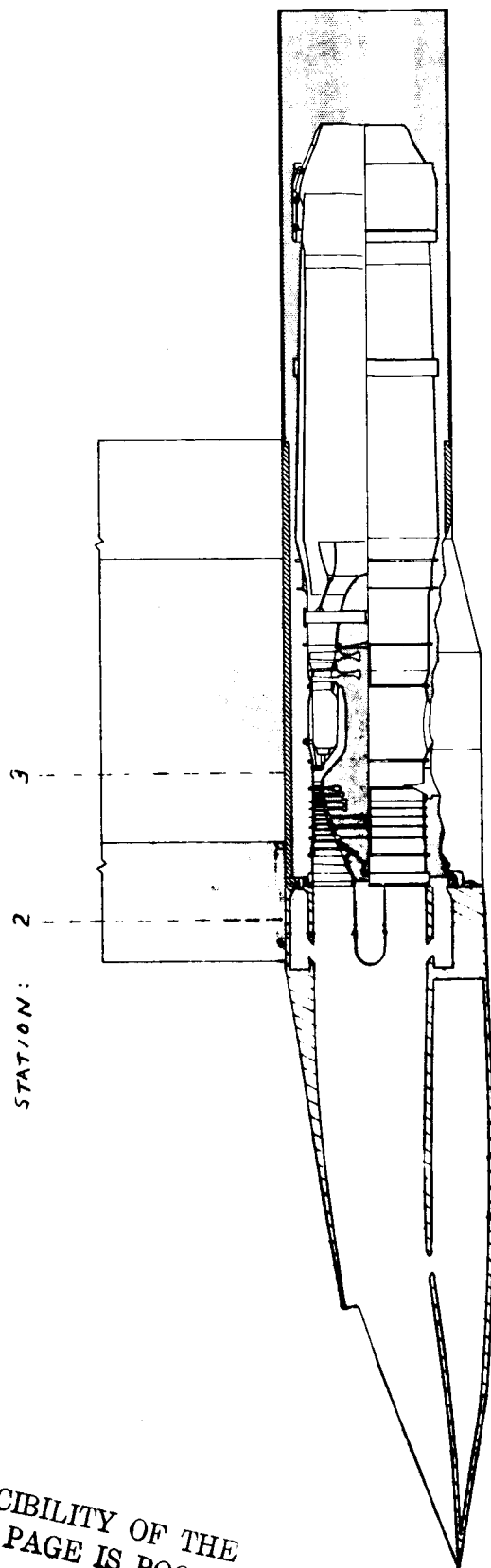


Figure 2. - Cutaway of nacelle showing installation of J85-GE-13  
turbojet engine.

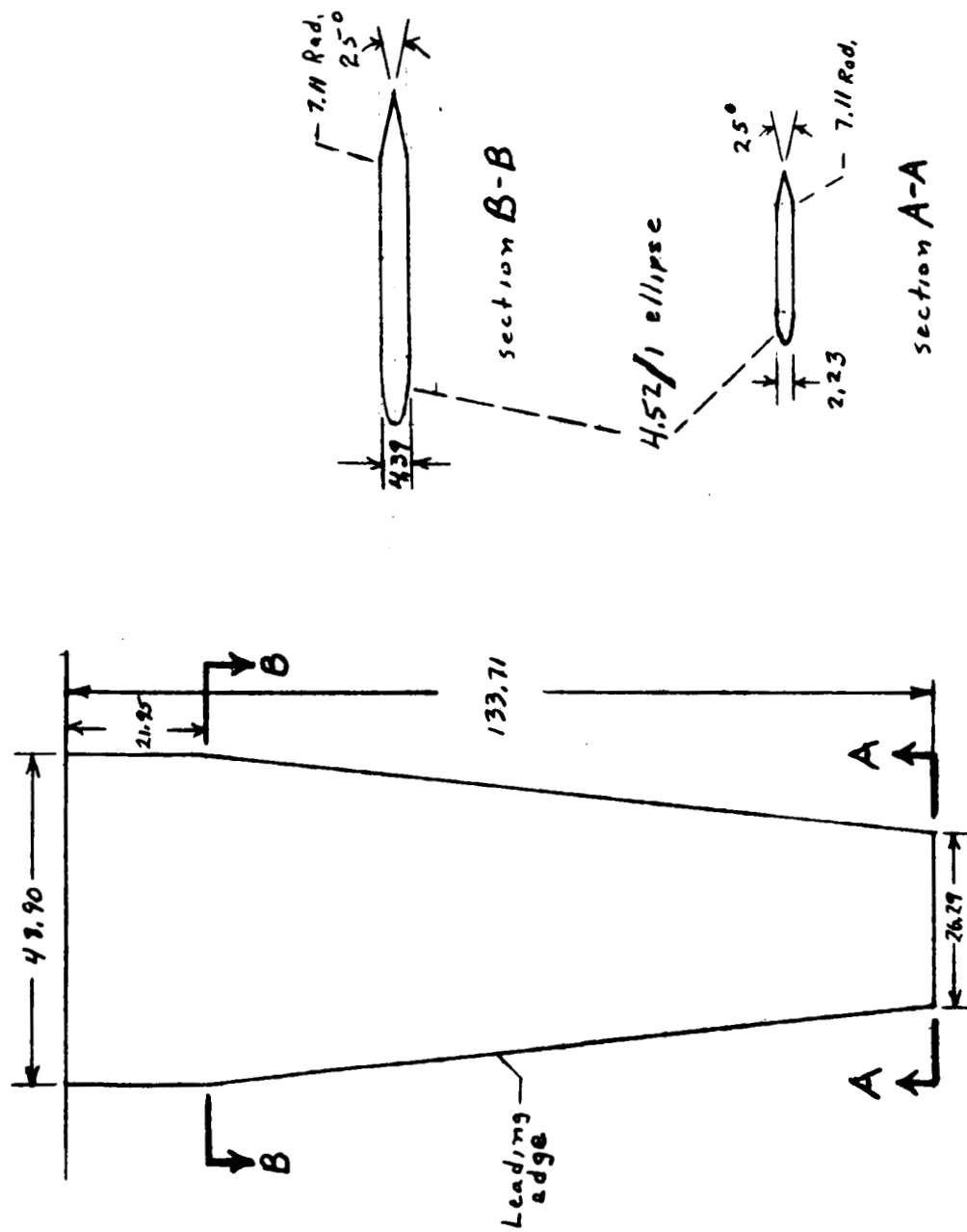


Figure 3.- Details of wing (All dimensions are in centimeters).

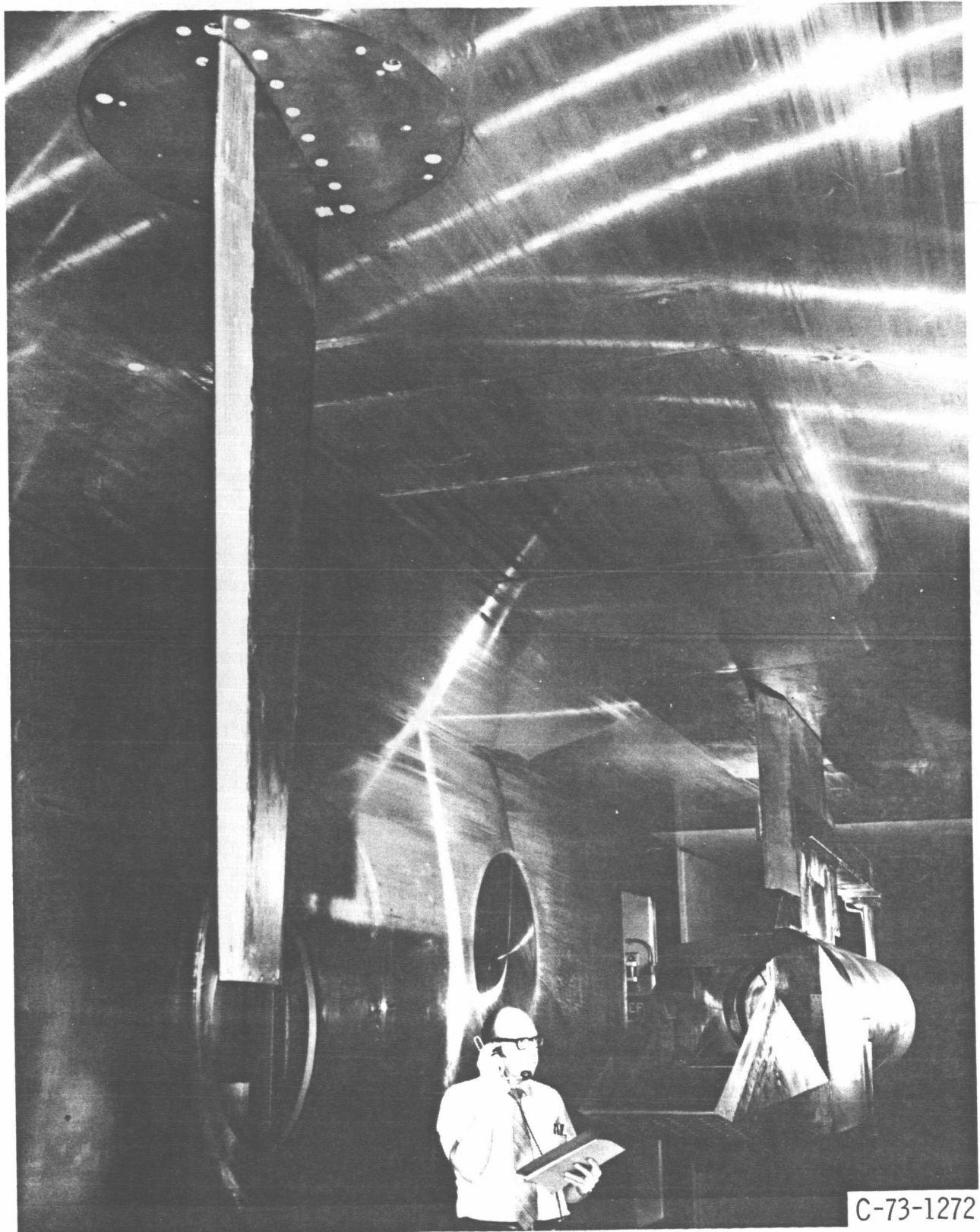


Figure 4. - Wing and inlet installed in 10- by 10-Foot Supersonic Wind Tunnel.

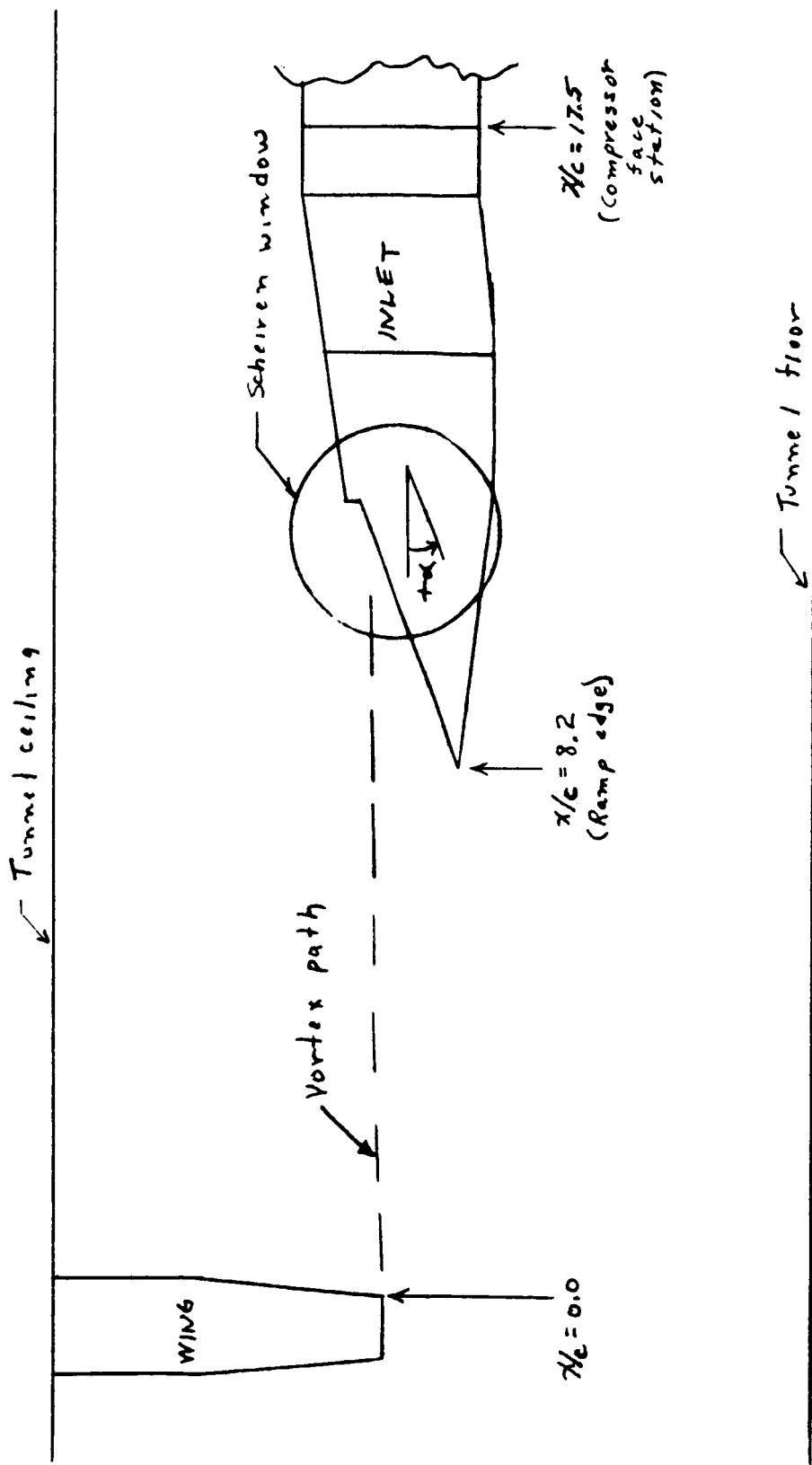


Figure 5. - Schematic of test set up.

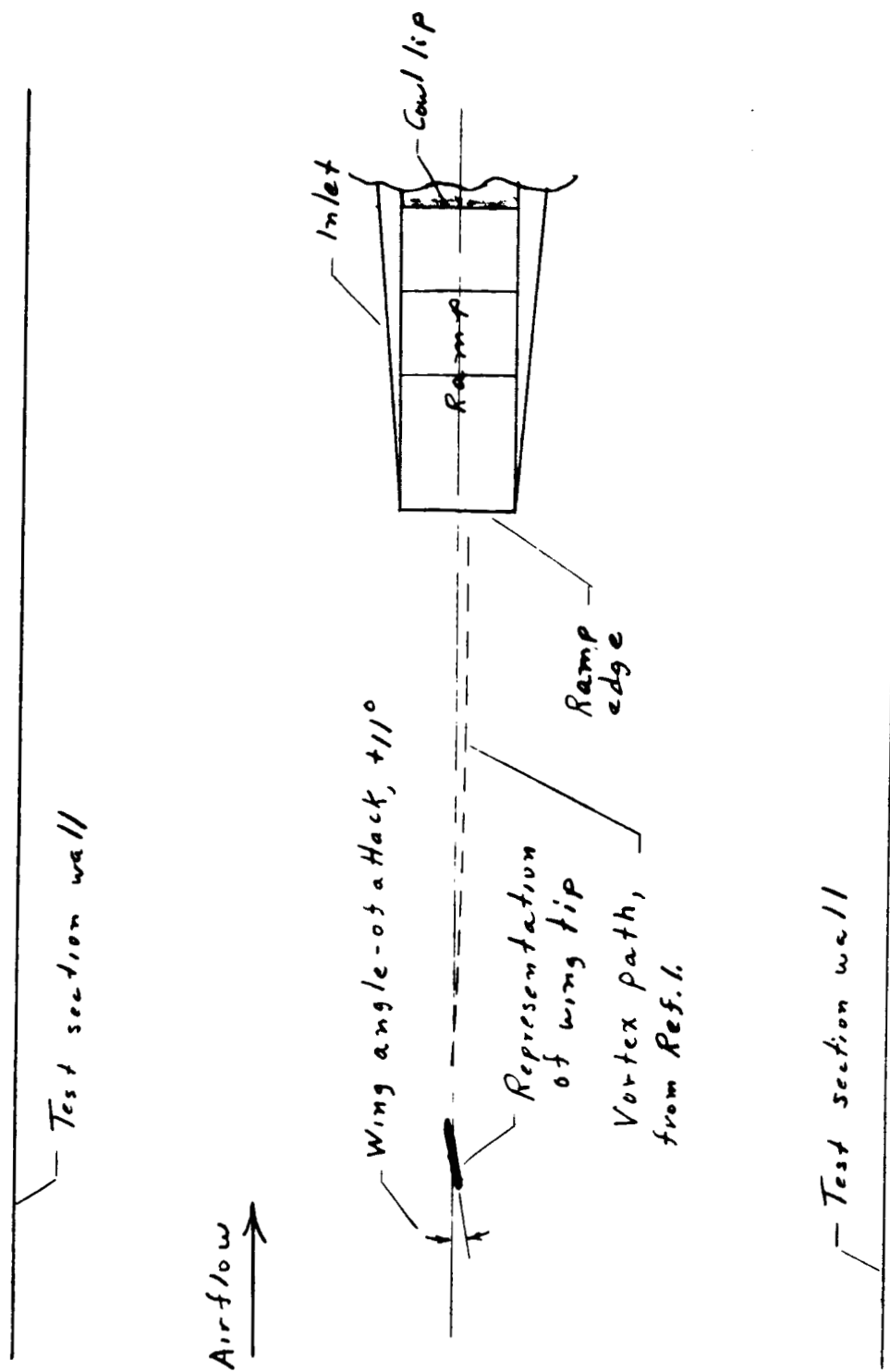
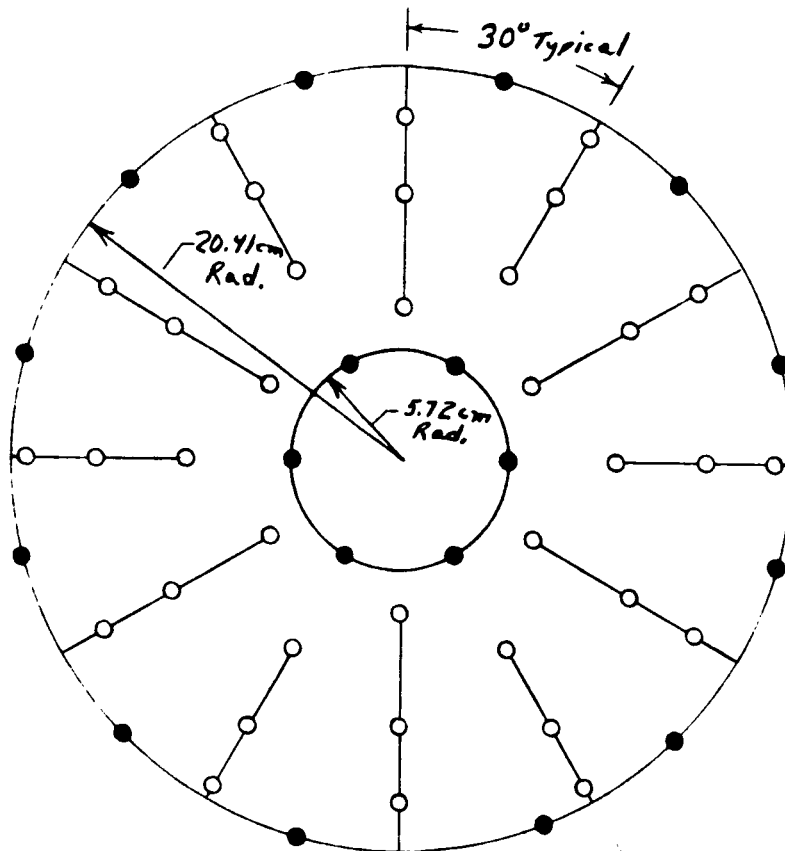


Figure 6.- Plan view of test set up.

- Total-pressure probe
- Static-pressure tap

Ramp side of compressor face



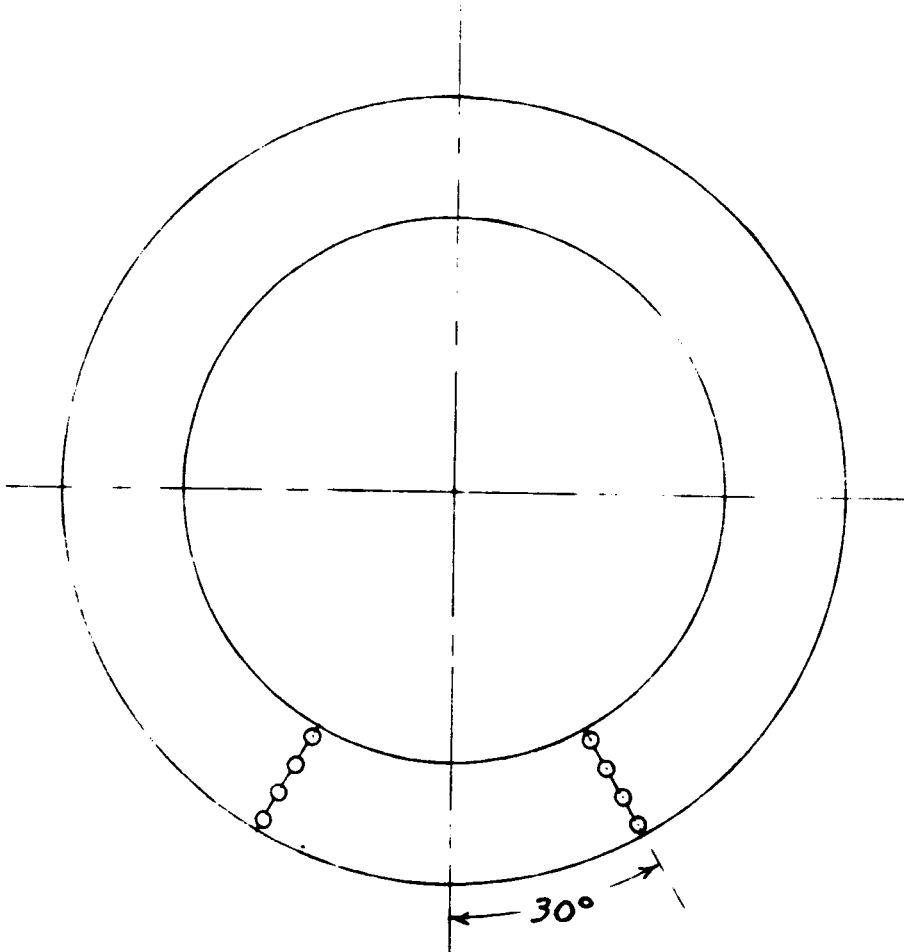
Cowl side of compressor face

Figure 7. - Compressor-face (station 2) instrumentation, looking downstream.



- Total-pressure probe

Ramp side of compressor exit



Cowl side of compressor exit

Figure 8.- J85-GE-13 engine compressor-exit  
(station 3) instrumentation.

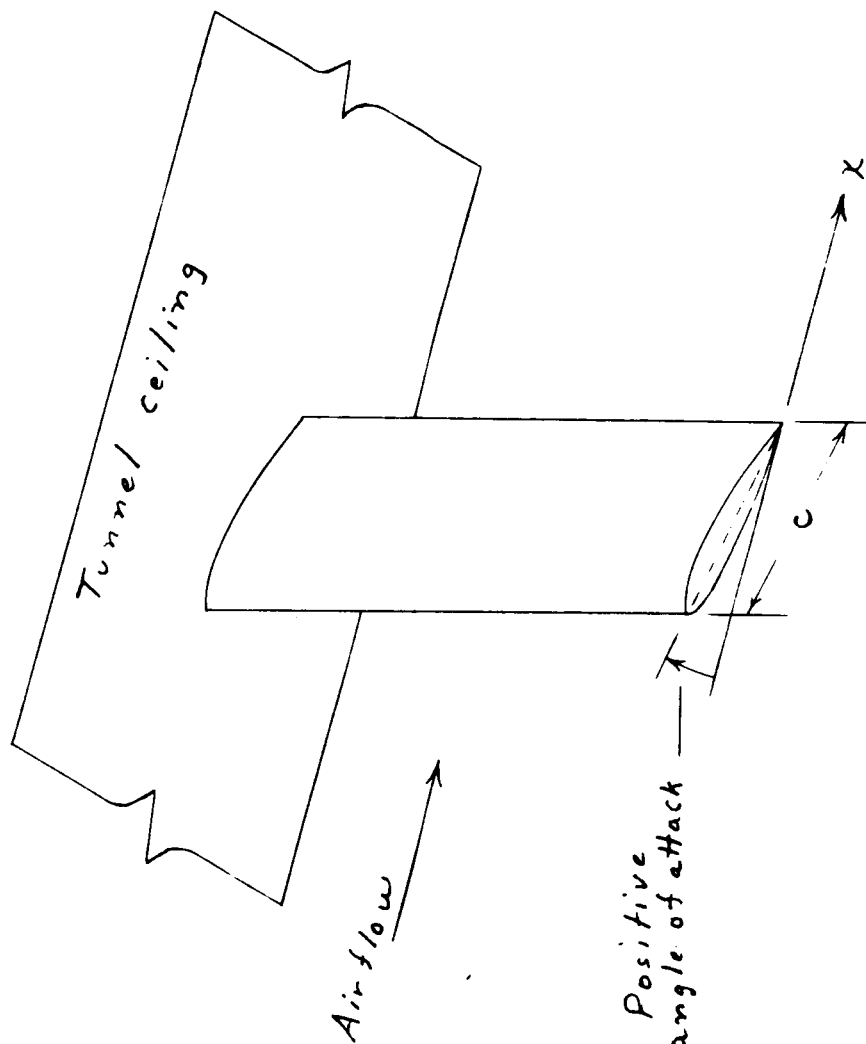
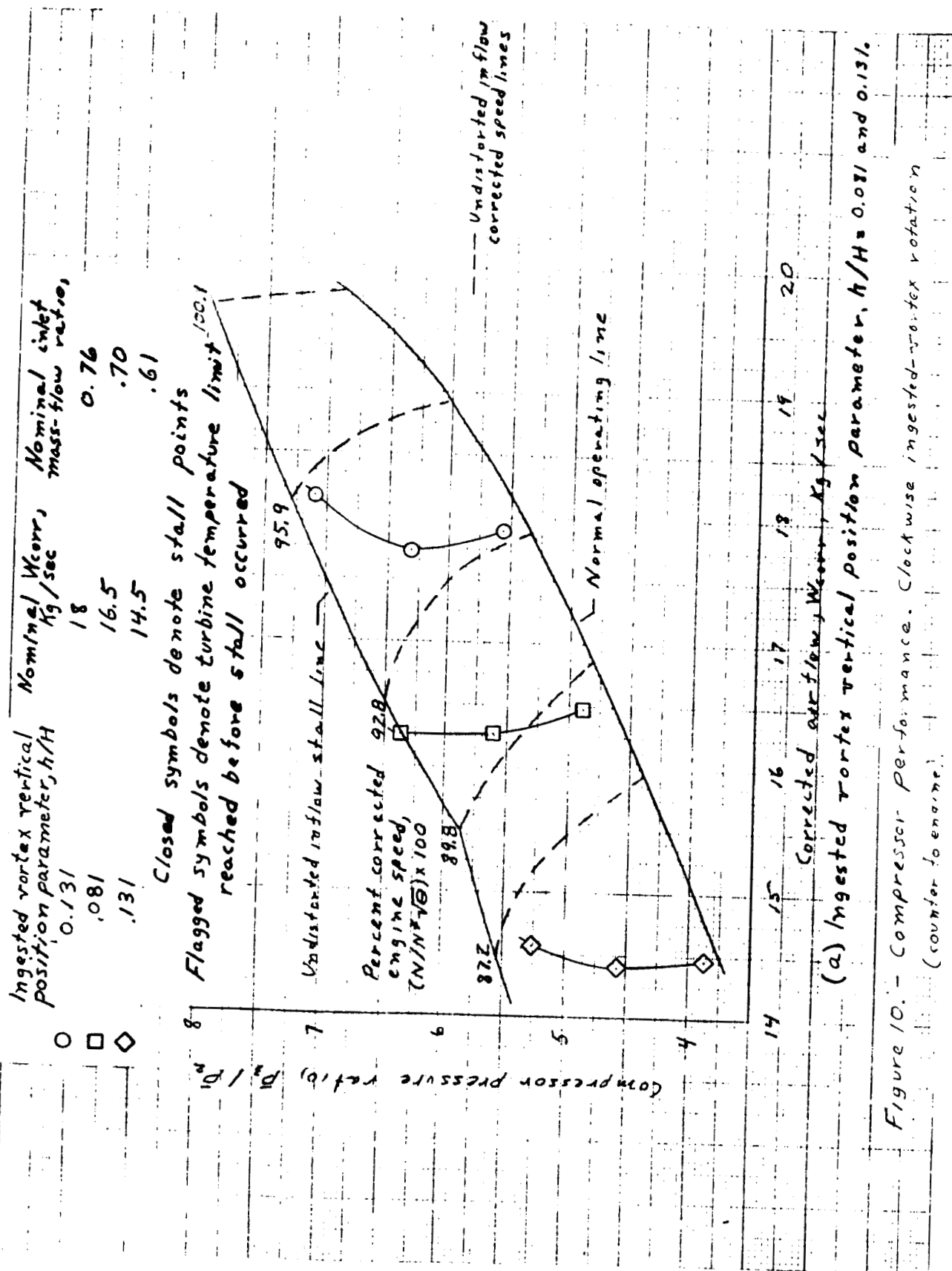


Figure 9.- Positive wing angle of attack.

REPRODUCIBILITY OF THE  
ORIGINAL PAGE IS POOR

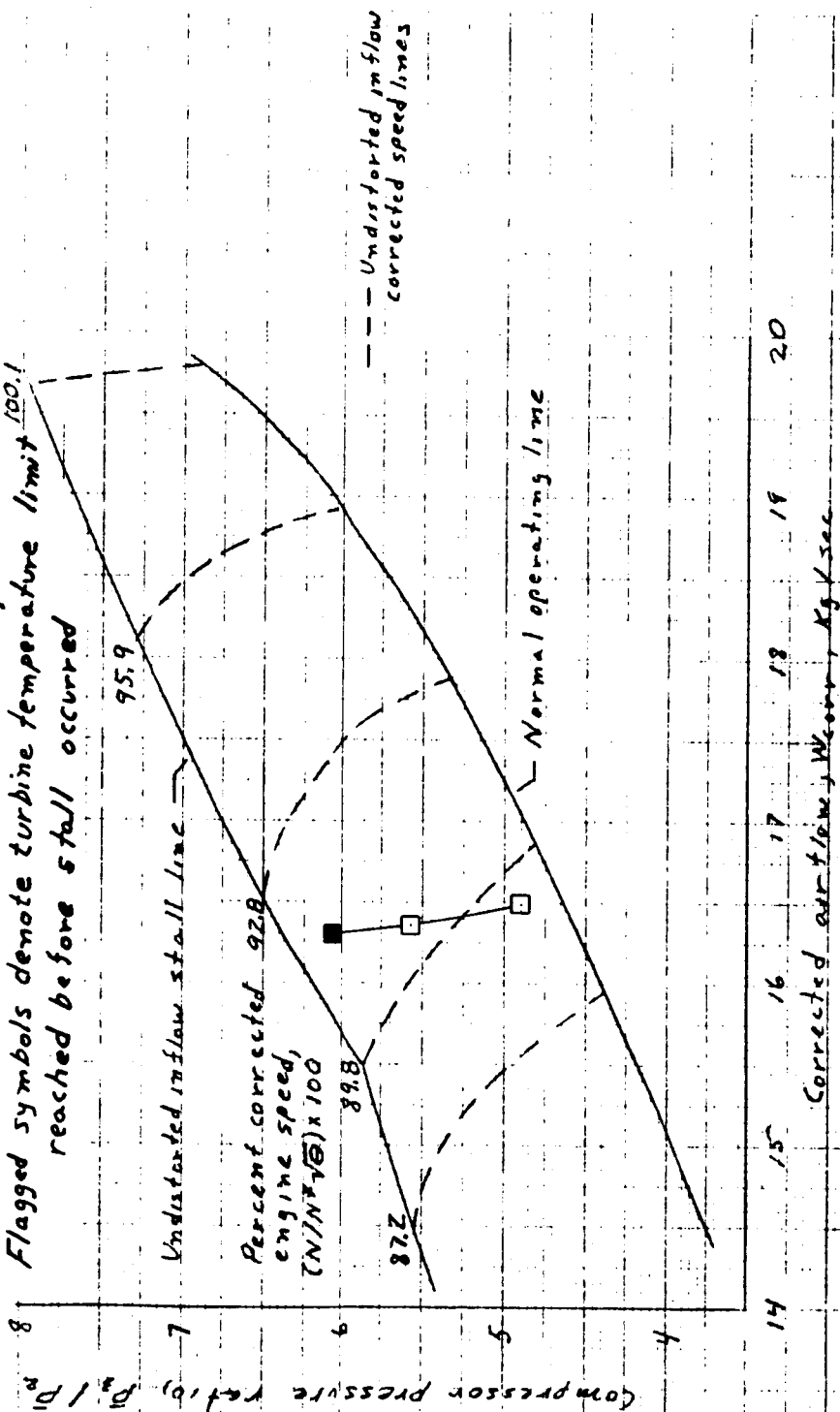


REPRODUCIBILITY OF THE ORIGINAL PAGE IS POOR

Nominal  $W_{corr}$ ,  $kg/sec$       Nominal inlet mass-flow ratio,

□      16.5      .70

Closed symbols denote stall points  
Flagged symbols denote turbine temperature limit reached before stall occurred



(b) Ingested vortex vertical position parameter,  $h/H = 0.194$ .

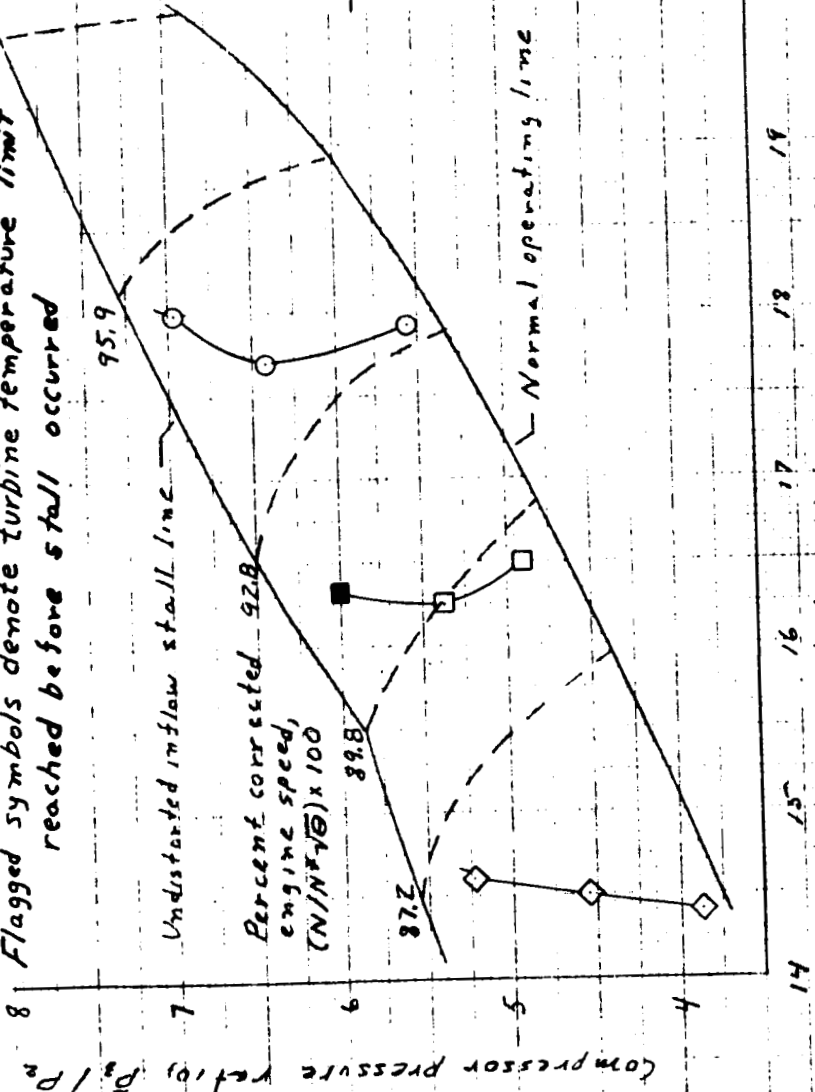
Figure 10.- Continued.

Nominal  $W_{corr}$ ,  $kg/sec$       Nominal inlet mass-flow ratio,

○ 18      0.76  
 □ 16.5      .70  
 ◇ 14.5      .61

Closed symbols denote stall points

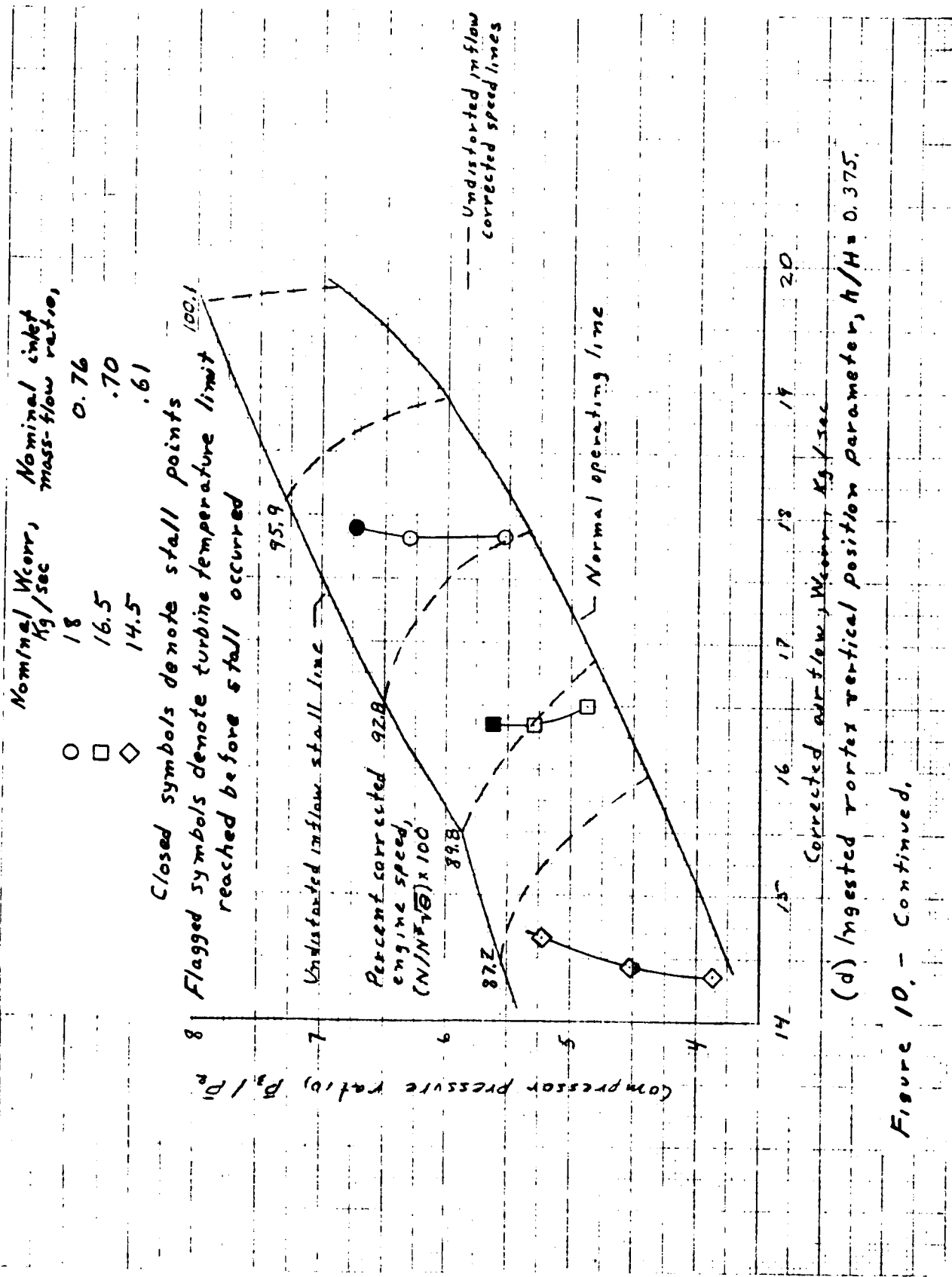
Flagged symbols denote turbine temperature limit reached before stall occurred



(c) Ingested vortex vertical position parameter,  $h/H = 0.244$ .

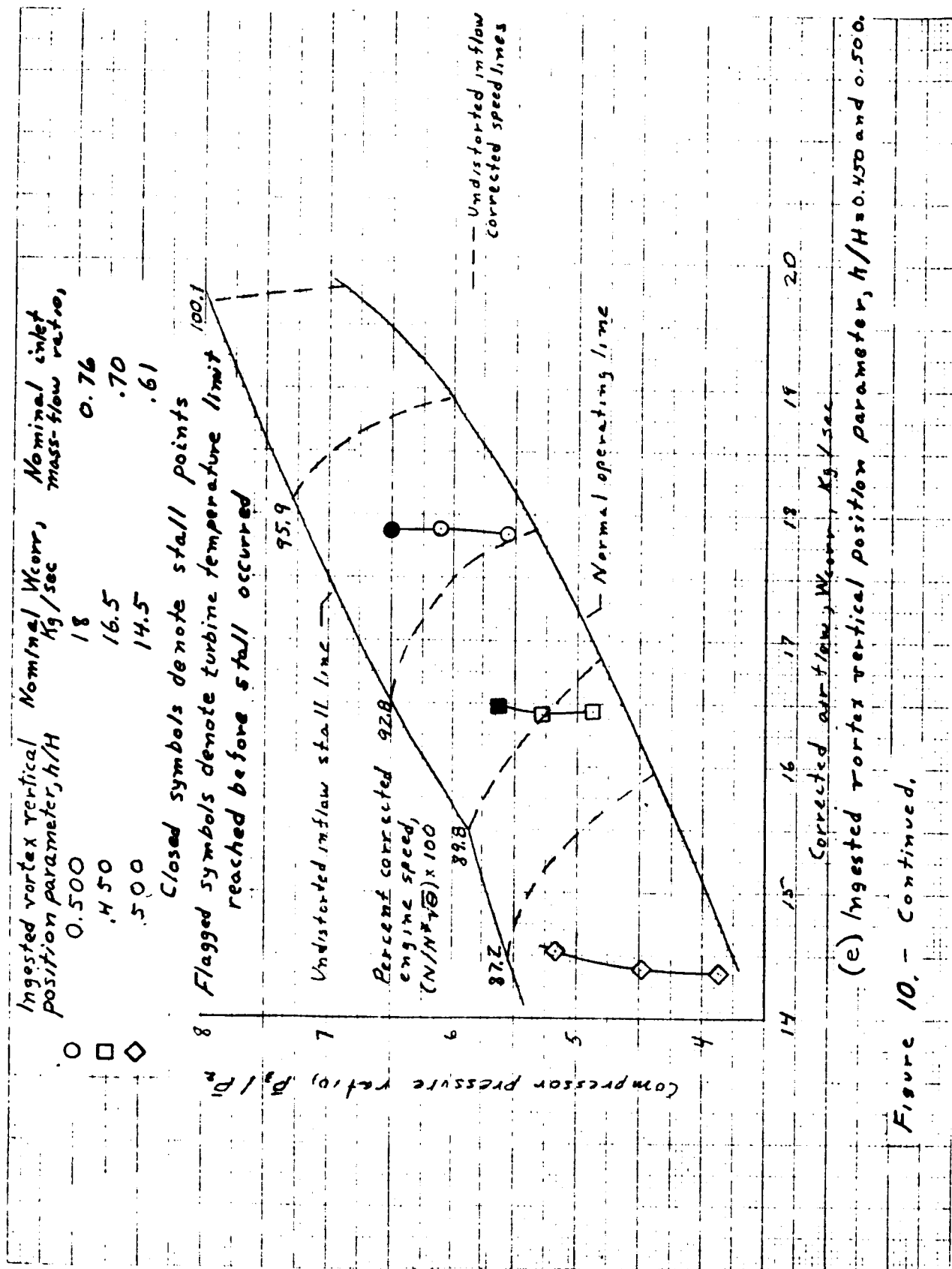
Figure 10. - Continued.

REPRODUCIBILITY OF THE ORIGINAL PAGE IS POOR



(d) Ingested vortex vertical position parameter,  $h/H = 0.375$ .

Figure 10, - Continued.



REPRODUCIBILITY OF THE  
ORIGINAL PAGE IS POOR

Ingested vortex vertical position parameter,  $h/H$

○ □ ◇

Nominal  $W_{corr}$ , kg/sec

18

16.5

14.5

Nominal inlet mass-flow ratio,  $\alpha$

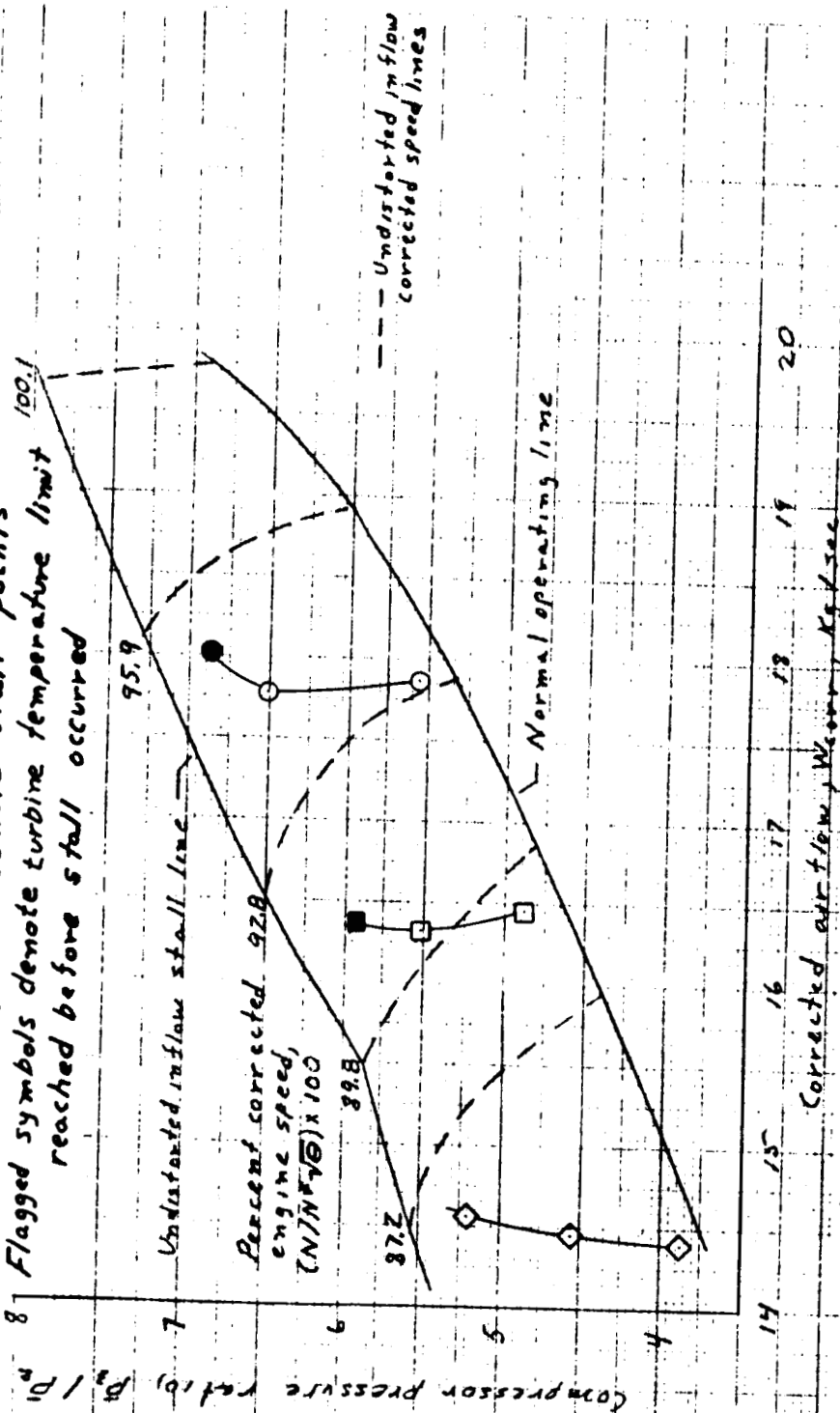
0.76

.70

.61

Closed symbols denote stall points

Flagged symbols denote turbine temperature limit reached before stall occurred



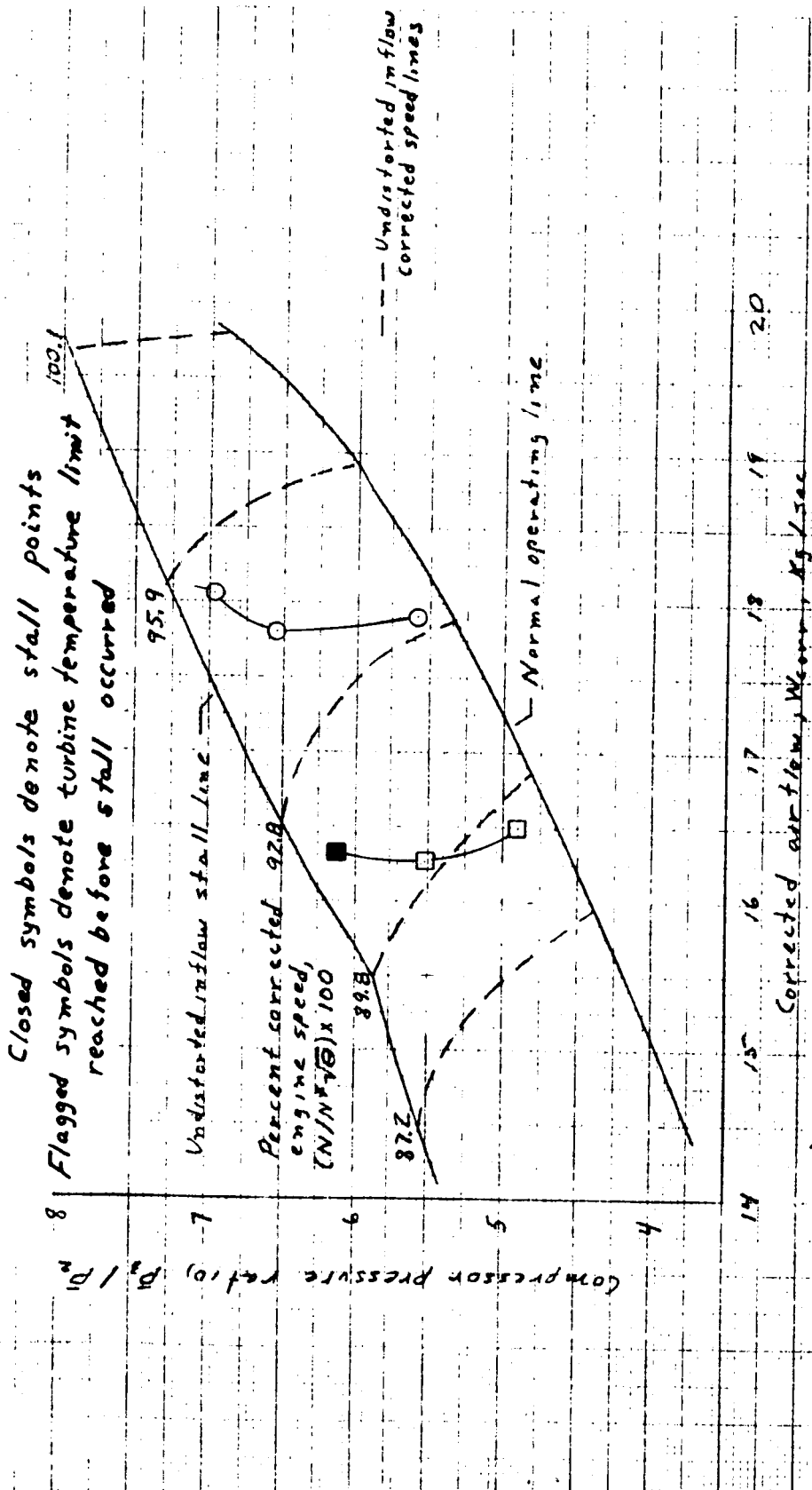
(f) Ingested vortex vertical position parameter,  $h/H = 0.575$  and  $0.625$ .

Figure 10. - Continued.

REPRODUCIBILITY OF THE  
ORIGINAL PAGE IS POOR

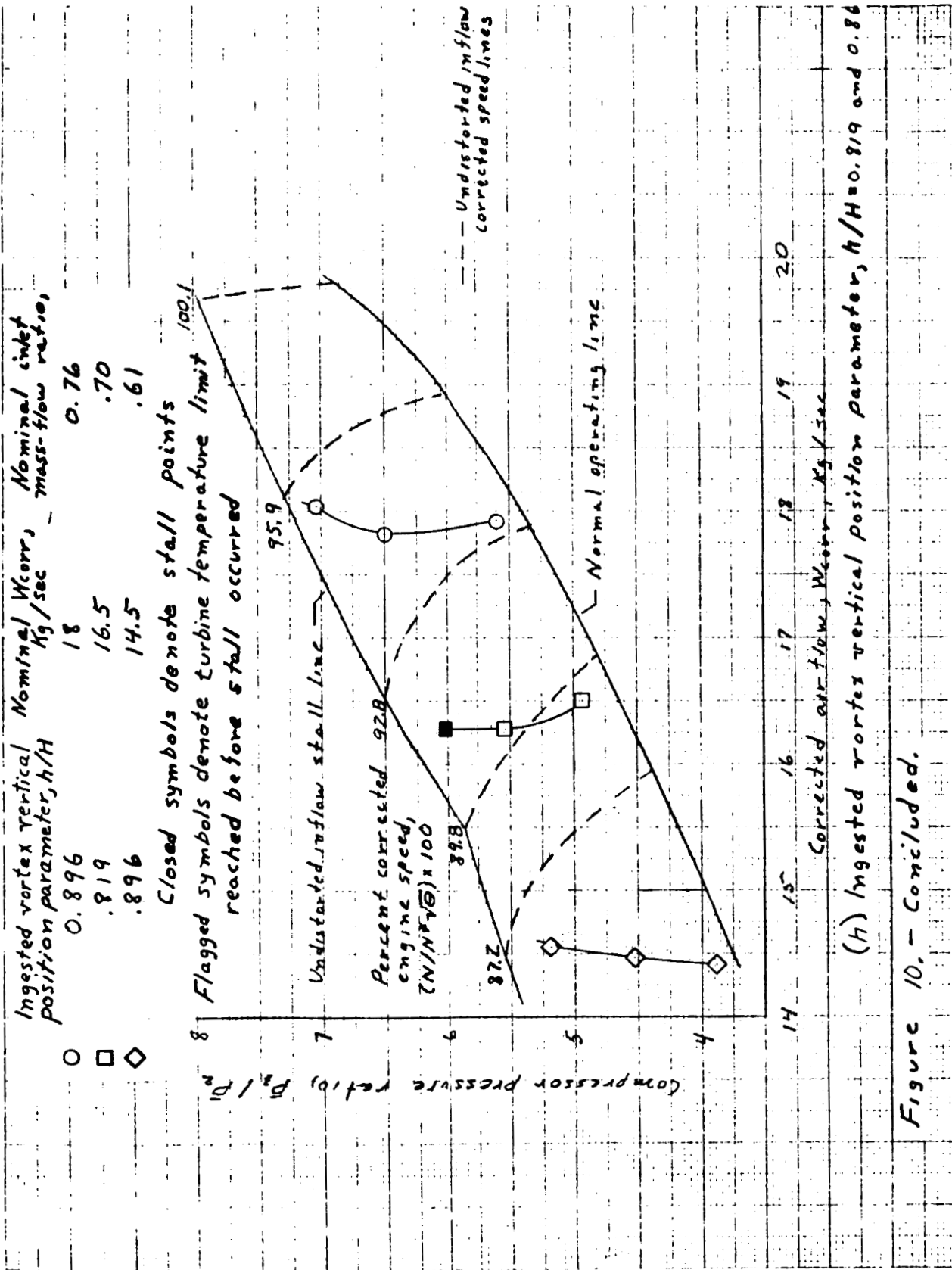


Ingested vortex vertical position parameter, $h/H$		Nominal $W_{corr}$ , $kg/sec$		Nominal inlet mass-flow ratio,	
○	0.756	18		0.76	
□	.706	16.5		.70	

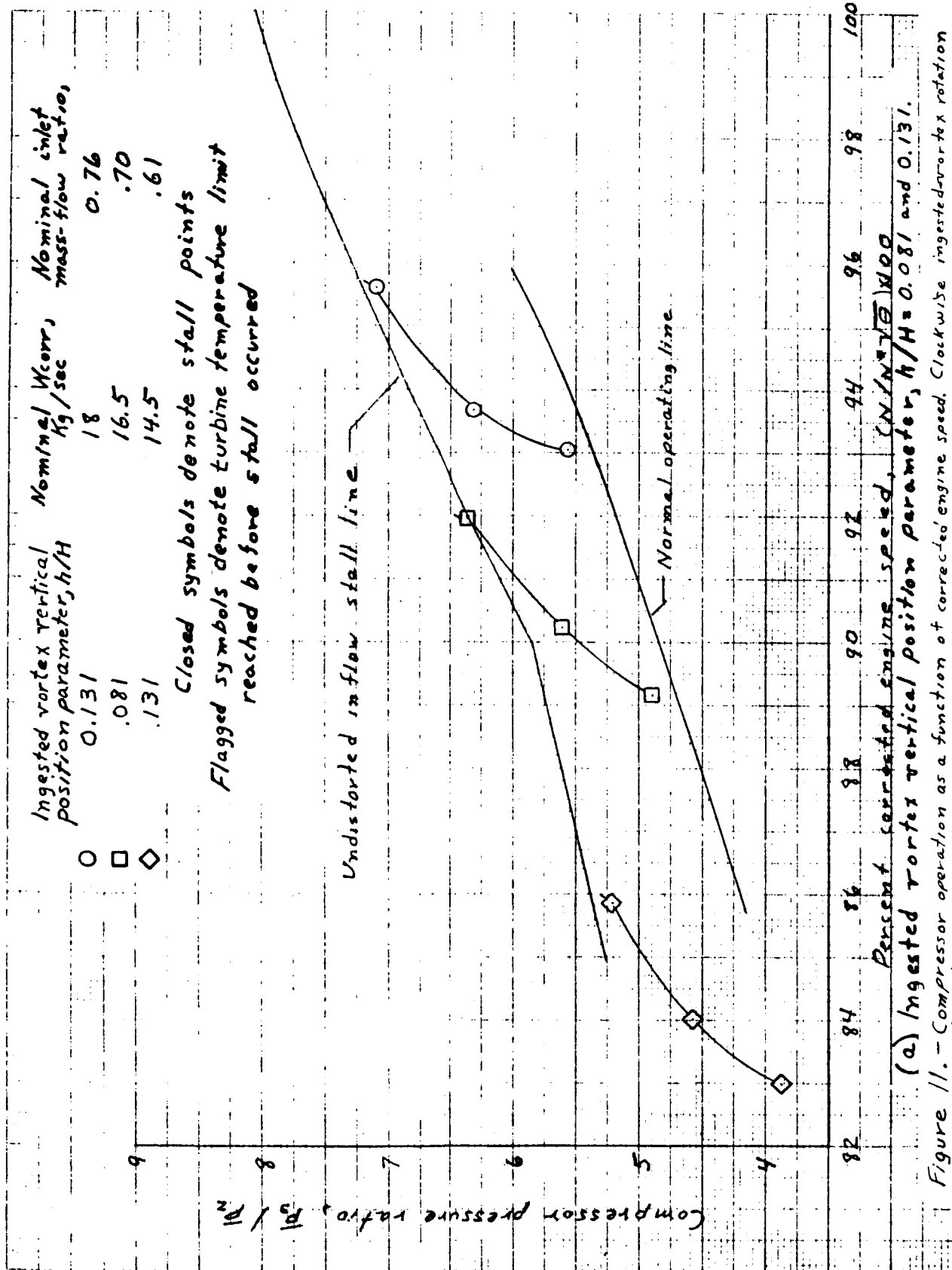


(9) Ingested vortex vertical position parameter,  $h/H=0.706$  and  $0.756$ .

Figure 10. - Continued.



REPRODUCIBILITY OF THE  
ORIGINAL PAGE IS POOR



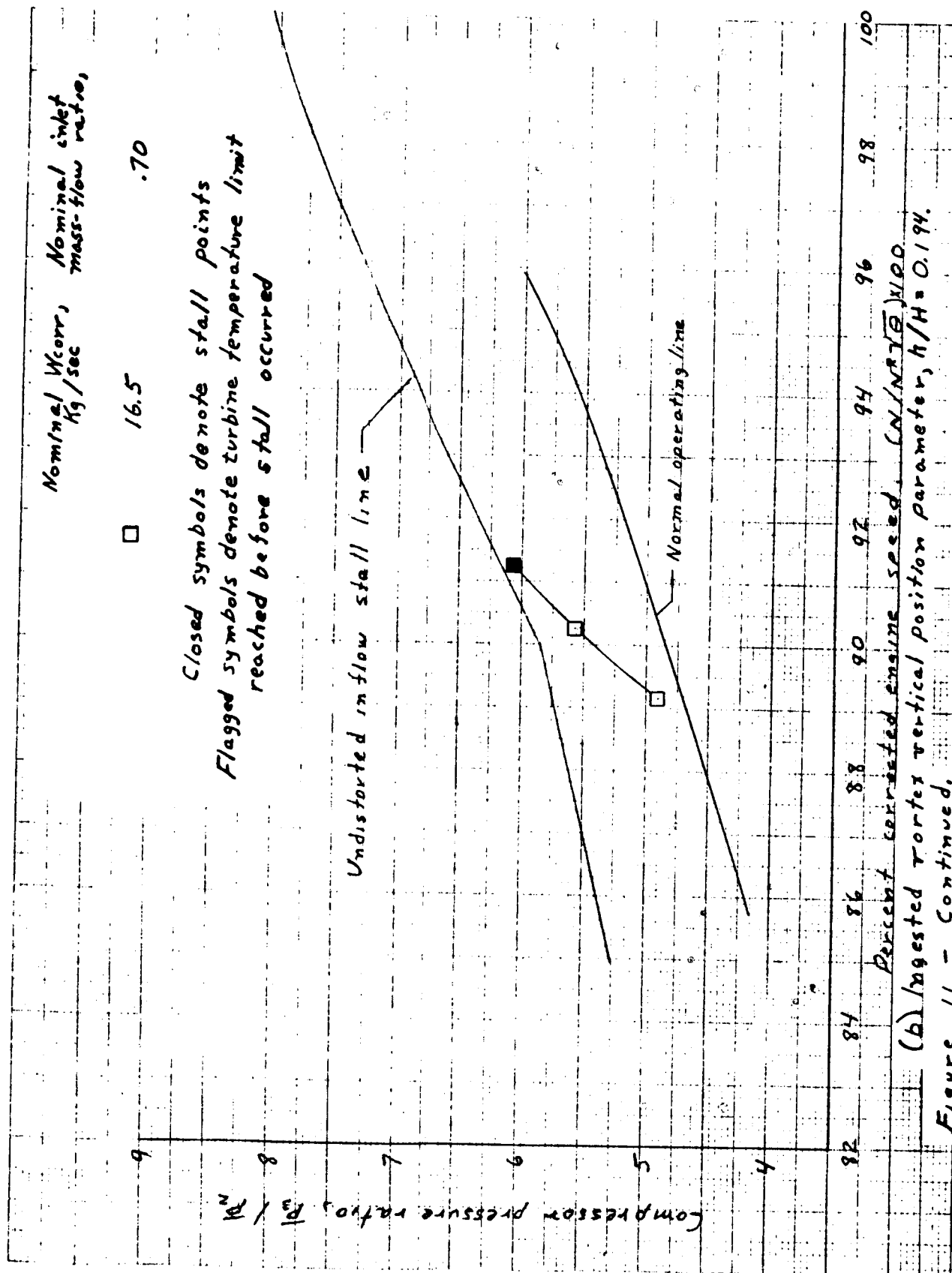


Figure 11. - Continued.

REPRODUCIBILITY OF THE  
ORIGINAL PAGE IS POOR

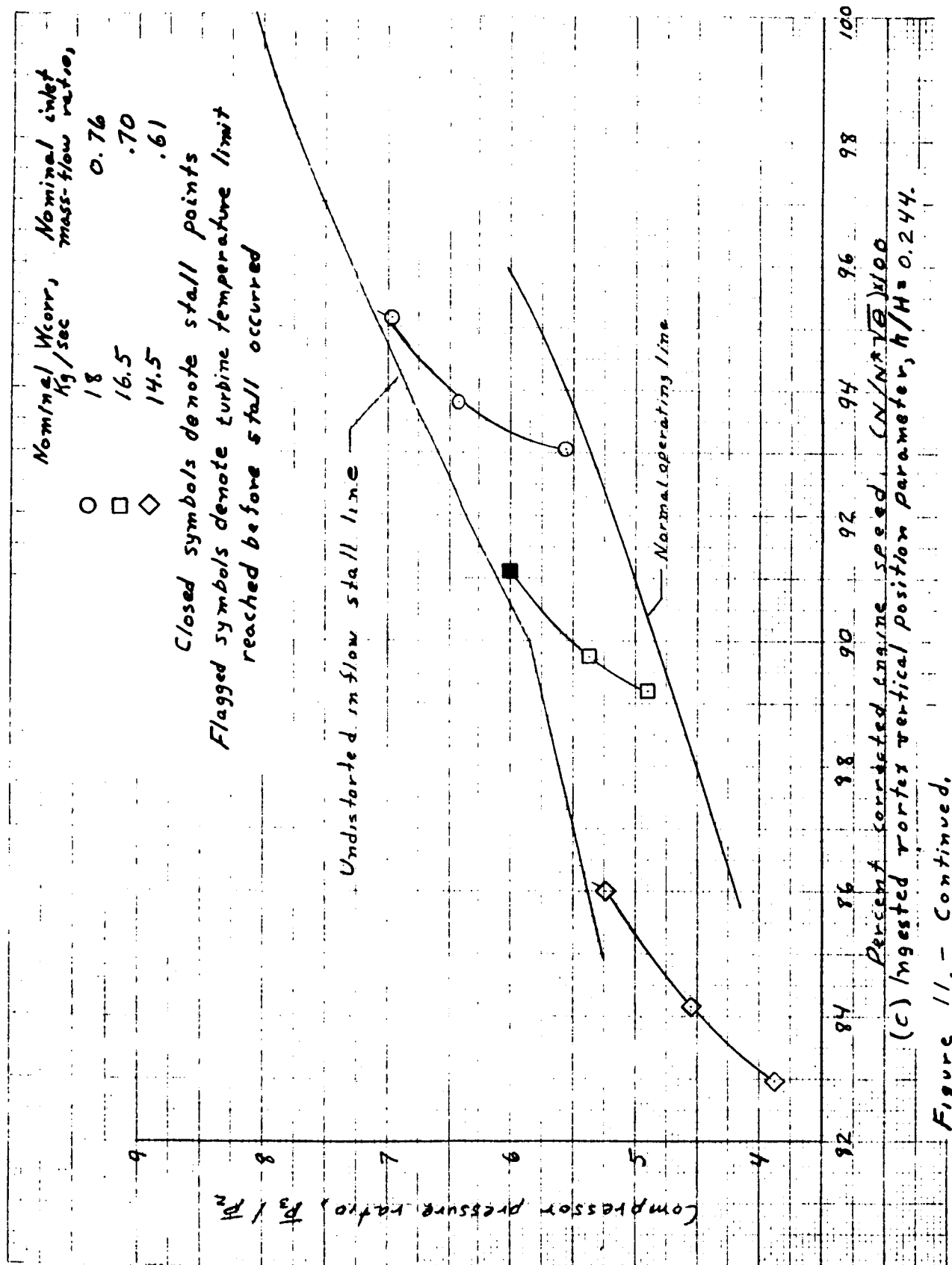
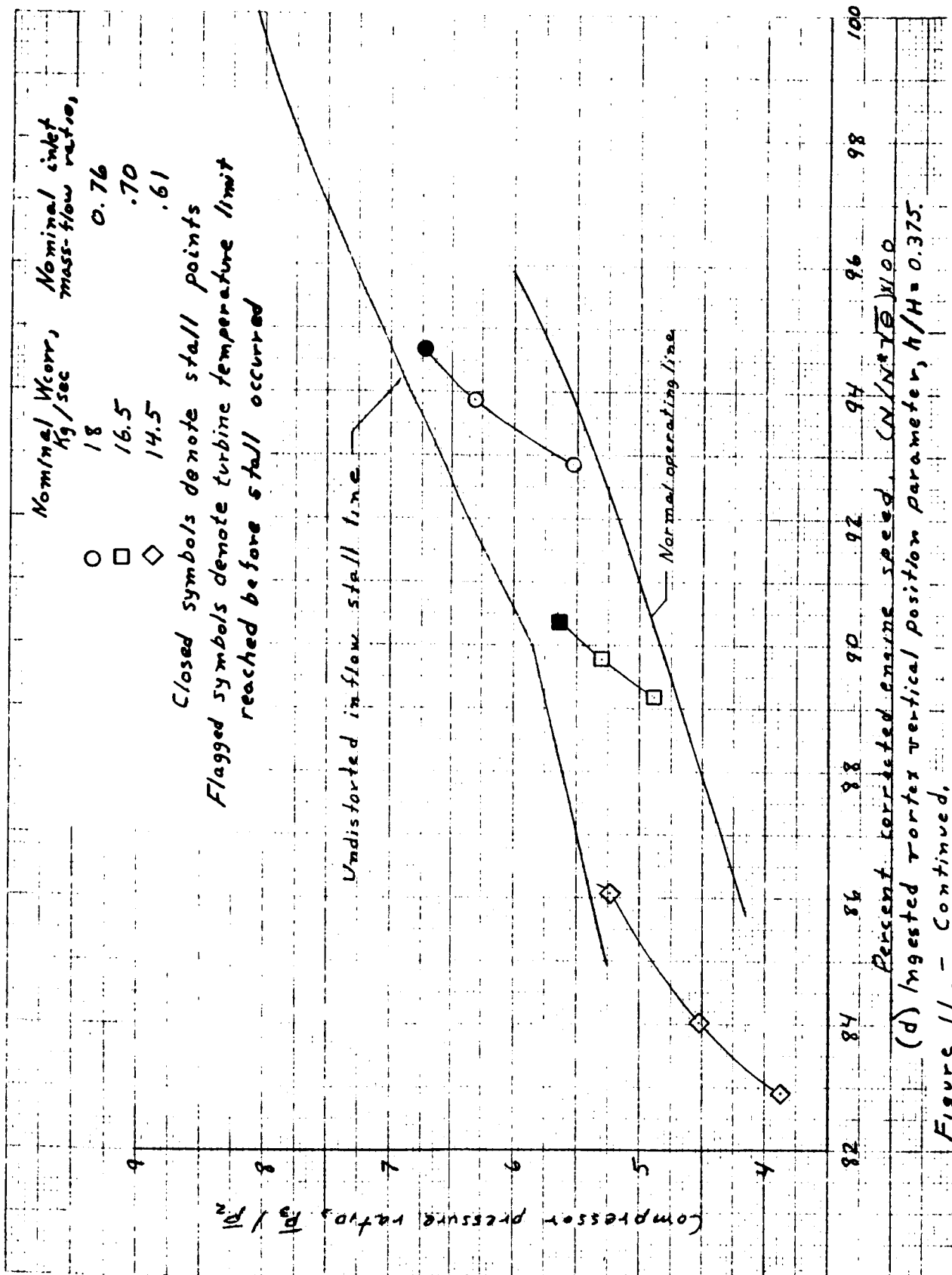


Figure 11. - Continued.



Ingested vortex vertical position parameter,  $h/H$

Nominal  $W_{corr}$ , kg/sec

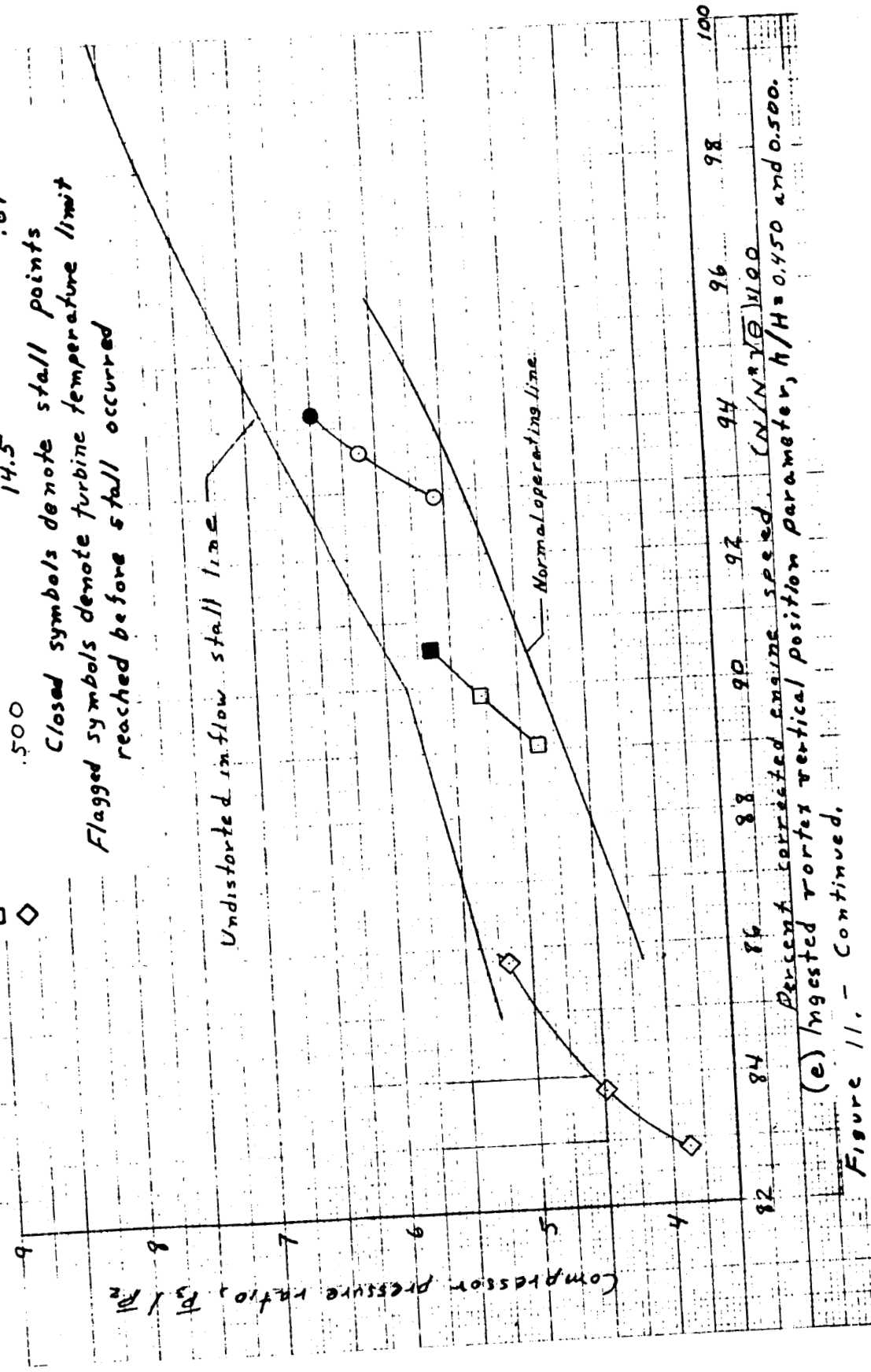
Nominal inlet mass-flow ratio,  $0.76$

0.500 18

.450 16.5

.500 14.5

Closed symbols denote stall points reached before stall occurred



(e) Ingested vortex vertical position parameter,  $h/H = 0.450$  and  $0.500$ .

Figure 11. - Continued.

REPRODUCIBILITY OF THE ORIGINAL PAGE IS POOR

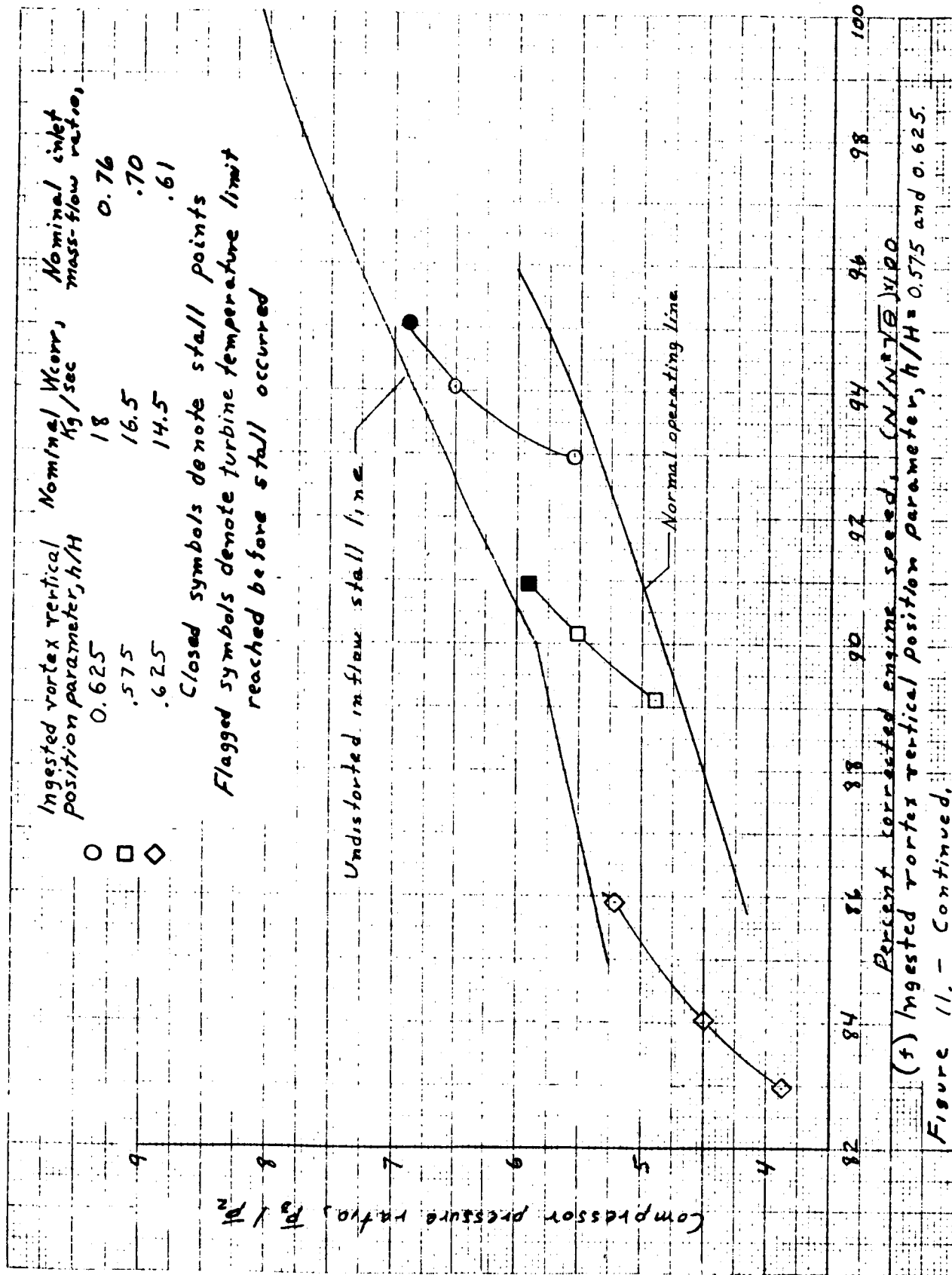
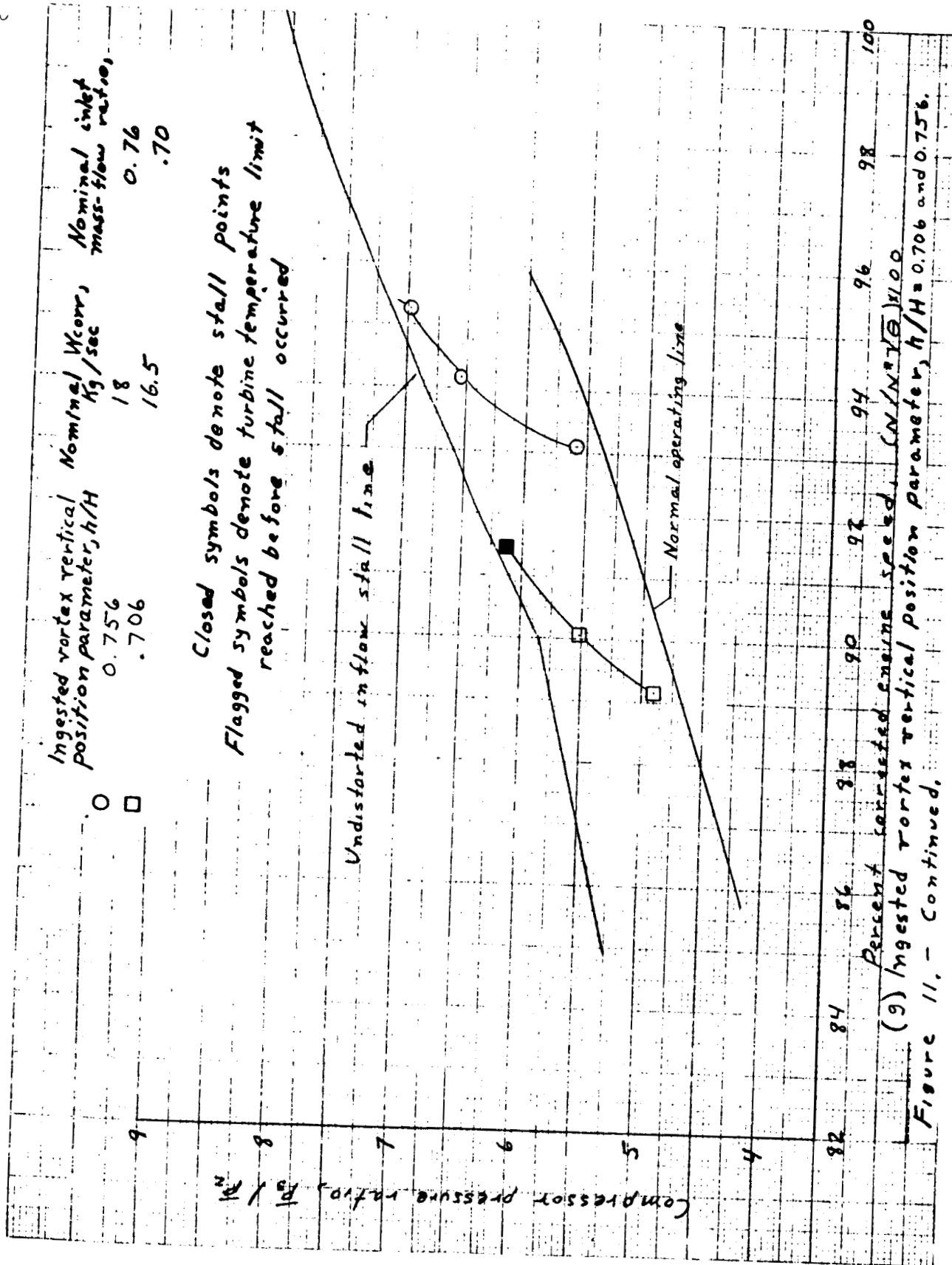


Figure 11. - Continued.





REPRODUCIBILITY OF THE  
ORIGINAL PAGE IS POOR

Ingested vortex vertical position parameter,  $h/H$

Nominal  $W_{corr}$ ,  $kg/sec$

Nominal inlet mass-flow ratio,

○ □ ◇

0.869  
.819  
.869

18  
16.5  
14.5

0.76  
.70  
.61

Closed symbols denote stall points reached before stall occurred

Undistorted inflow stall line

Normal operating line

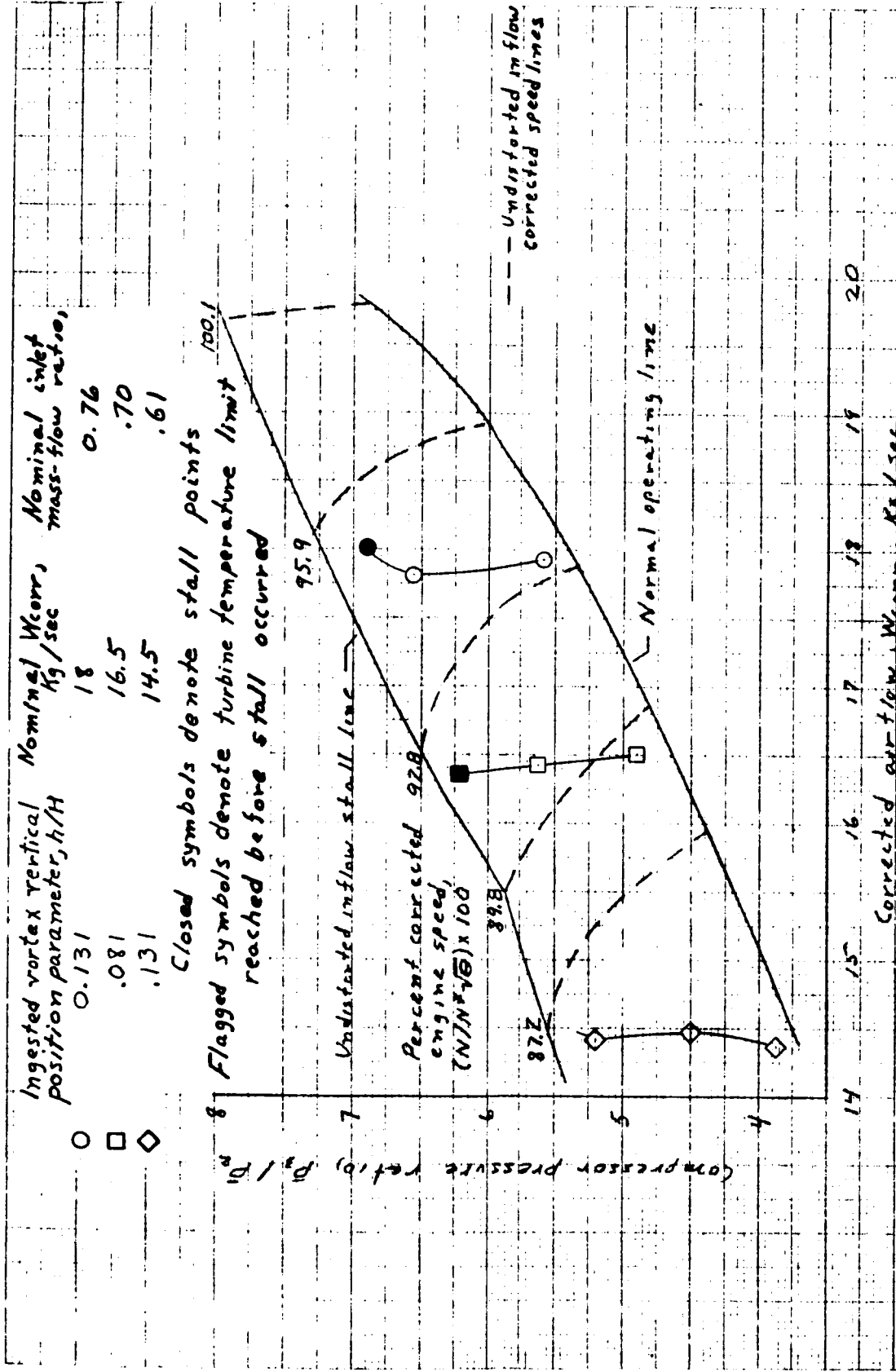
Compressor pressure ratio,  $P_3/P_2$

82 84 86 88 90 92 94 96 98 100

Percent corrected engine speed,  $(N/N^*)\sqrt{\theta}$

(h) Ingested vortex vertical position parameter,  $h/H = 0.819$  and  $0.869$

Figure 11, - Concluded.



(a) Ingested vortex vertical position parameter,  $h/H = 0.08$  and  $0.131$ .

Figure 12. - Compressor performance. Counterclockwise ingested-vortex rotation (with engine)

Nominal  $W_{corr}$ ,  $kg/sec$  Nominal inlet mass-flow ratio,

□ 16.5 .70

Closed symbols denote stall points  
Flagged symbols denote turbine temperature limit reached before stall occurred

100.1

95.9

Undistorted inflow stall line

Percent corrected engine speed,  $(N/N^* \sqrt{\theta}) \times 100$

92.8

86.8

Undistorted inflow corrected speed lines

Normal operating line

Compressor pressure ratio,  $P_2/P_1$

14 15 16 17 18 19 20

Corrected air flow,  $W_{corr}$ ,  $kg/sec$

(b) Ingested vortex vertical position parameter,  $h/H = 0.194$ .

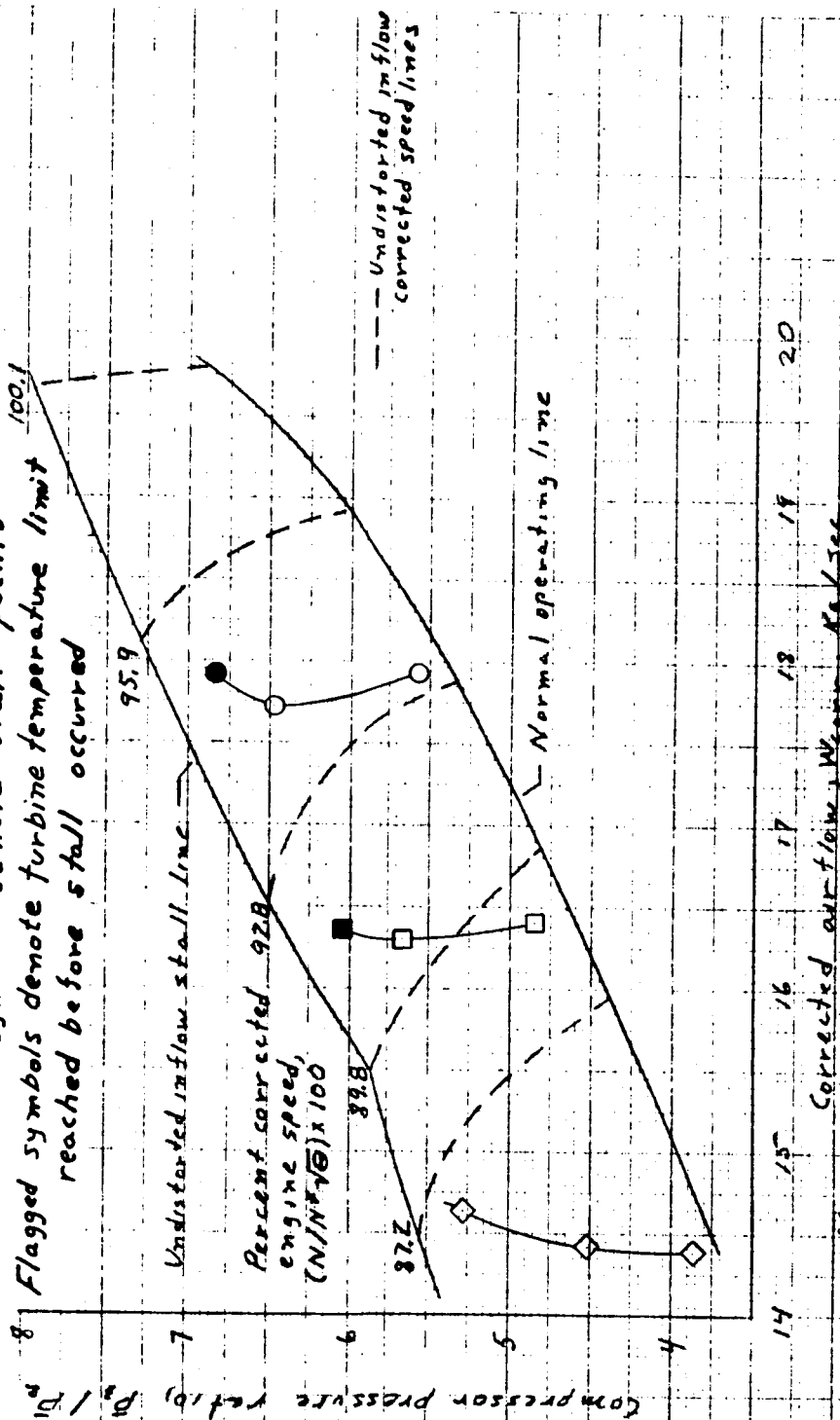
Figure 12, - Continued.

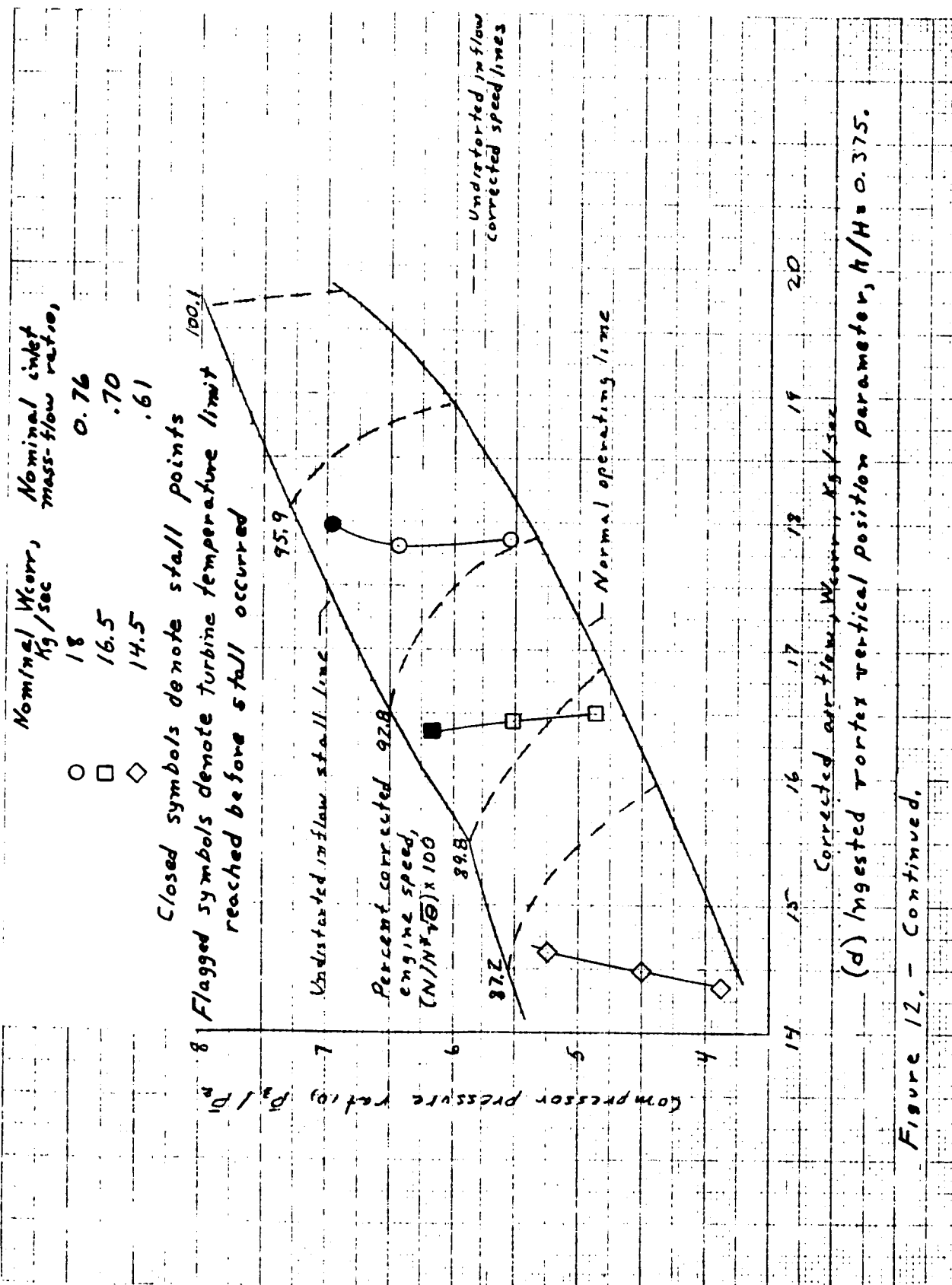
REPRODUCIBILITY OF THE ORIGINAL PAGE IS POOR

Nominal  $W_{corr}$ ,  $kg/sec$       Nominal inlet mass-flow ratio,

○ 18      0.76  
 □ 16.5      .70  
 ◇ 14.5      .61

Closed symbols denote stall points  
 Flagged symbols denote turbine temperature limit reached before stall occurred





REPRODUCIBILITY OF THE  
ORIGINAL PAGE IS POOR

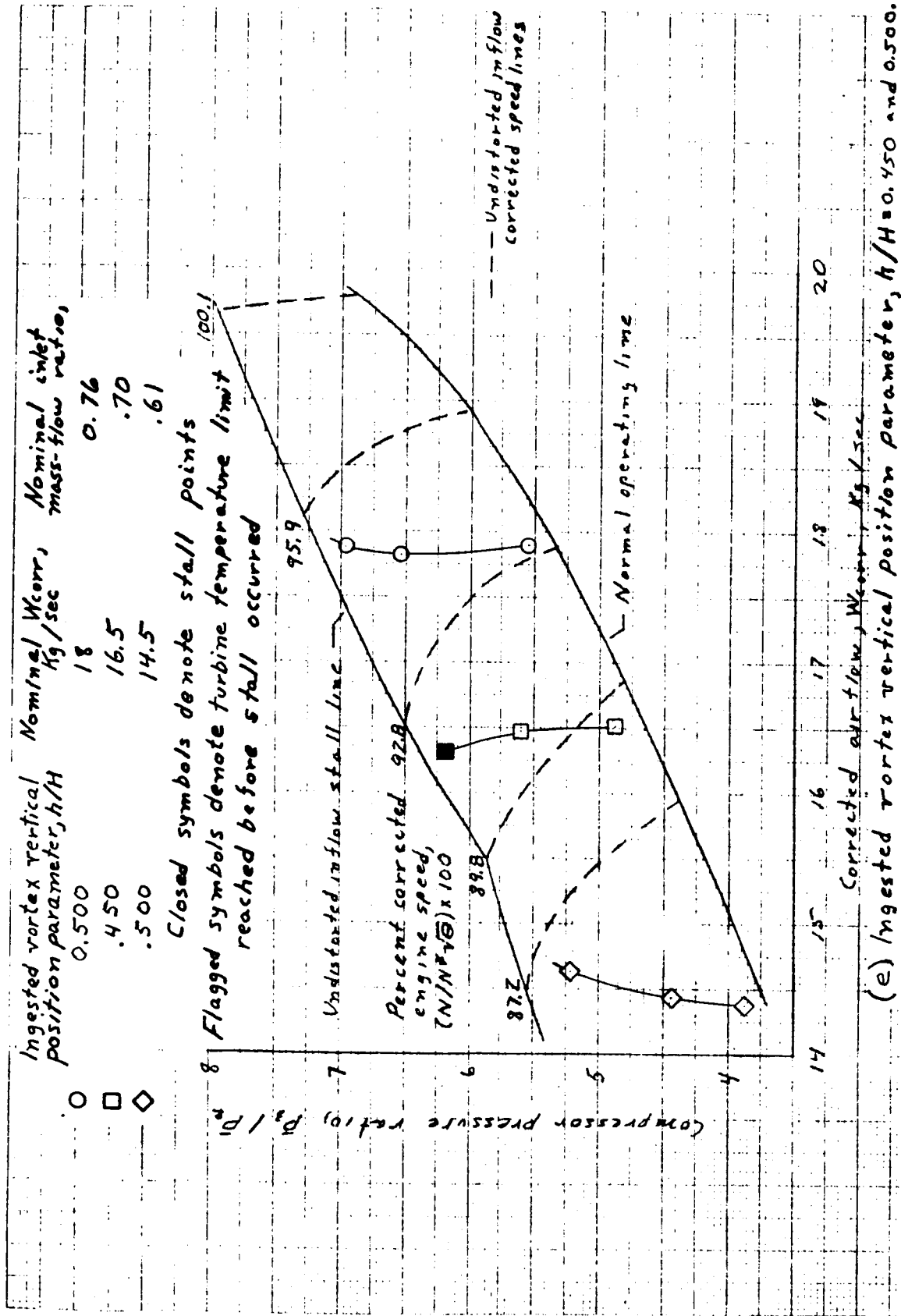


Figure 12. - Continued.

Ingested vortex vertical position parameter,  $h/H$

Nominal  $W_{corr}$ , kg/sec

Nominal inlet mass-flow ratio,

○

□

◇

0.625

0.76

.575

16.5

.70

.625

14.5

.61

Closed symbols denote stall points

Flagged symbols denote turbine temperature limit reached before stall occurred

8

7

6

5

4

3

2

1

0

-1

-2

-3

-4

-5

-6

-7

-8

-9

-10

-11

-12

-13

-14

-15

-16

-17

-18

-19

-20

-21

-22

-23

-24

-25

-26

-27

-28

-29

-30

-31

-32

-33

-34

-35

-36

-37

-38

-39

-40

-41

-42

-43

-44

-45

-46

-47

-48

-49

-50

-51

-52

-53

-54

-55

-56

-57

-58

-59

-60

-61

-62

-63

-64

-65

-66

-67

-68

-69

-70

-71

-72

-73

-74

-75

-76

-77

-78

-79

-80

-81

-82

-83

-84

-85

-86

-87

-88

-89

-90

-91

-92

-93

-94

-95

-96

-97

-98

-99

-100

-101

-102

-103

-104

-105

-106

-107

-108

-109

-110

-111

-112

-113

-114

-115

-116

-117

-118

-119

-120

-121

-122

-123

-124

-125

-126

-127

-128

-129

-130

-131

-132

-133

-134

-135

-136

-137

-138

-139

-140

-141

-142

-143

-144

-145

-146

-147

-148

-149

-150

-151

-152

-153

-154

-155

-156

-157

-158

-159

-160

-161

-162

-163

-164

-165

-166

-167

-168

-169

-170

-171

-172

-173

-174

-175

-176

-177

-178

-179

-180

-181

-182

-183

-184

-185

-186

-187

-188

-189

-190

-191

-192

-193

-194

-195

-196

-197

-198

-199

-200

-201

-202

-203

-204

-205

-206

-207

-208

-209

-210

-211

-212

-213

-214

-215

-216

-217

-218

-219

-220

-221

-222

-223

-224

-225

-226

-227

-228

-229

-230

-231

-232

-233

-234

-235

-236

-237

-238

-239

-240

-241

-242

-243

-244

-245

-246

-247

-248

-249

-250

-251

-252

-253

-254

-255

-256

-257

-258

-259

-260

-261

-262

-263

-264

-265

-266

-267

-268

-269

-270

-271

-272

-273

-274

-275

-276

-277

-278

-279

-280

-281

-282

-283

-284

-285

-286

-287



Ingested vortex vertical position parameter,  $h/H$

○ □

0.756  
.706

Nominal  $W_{corr}$ ,  $kg/sec$

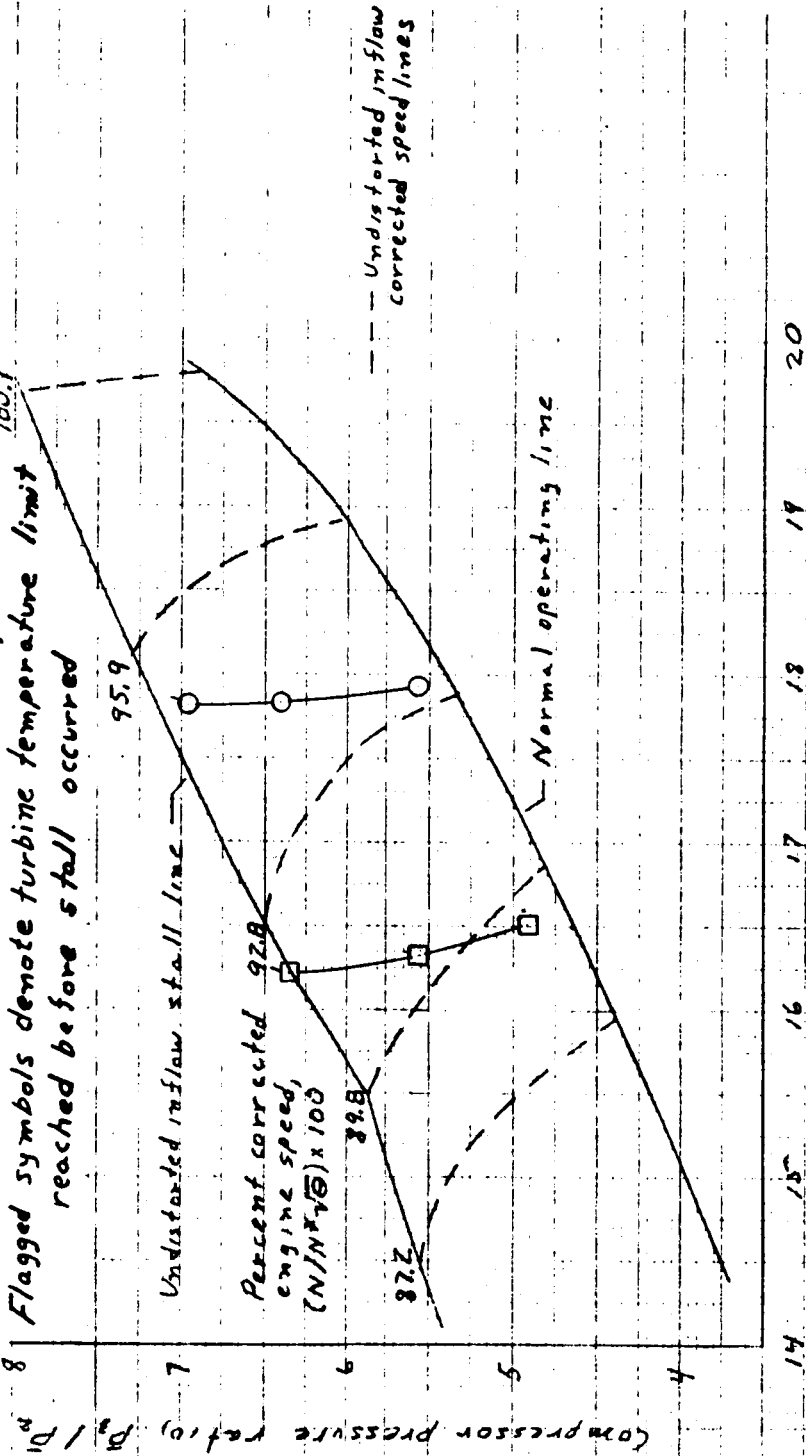
18  
16.5

Nominal inlet mass-flow ratio,

0.76  
.70

Closed symbols denote stall points

Flagged symbols denote turbine temperature limit reached before stall occurred



(9) Ingested vortex vertical position parameter,  $h/H=0.706$  and  $0.756$ .

Figure 12. - Continued.

Ingested vortex vertical position parameter,  $h/H$

Nominal  $W_{corr}$ ,  $kg/sec$

Nominal inlet mass-flow ratio,

0.869  
0.819  
0.869

18  
16.5  
14.5

0.76  
.70  
.61

Closed symbols denote stall points

Flagged symbols denote turbine temperature limit reached before stall occurred

100.1

95.9

92.8

88.8

82.8

72.8

62.8

52.8

42.8

Undistorted inflow stall line

Percent corrected engine speed,  $(N/N_{T0}) \times 100$

Undistorted inflow corrected speed lines

Normal operating line

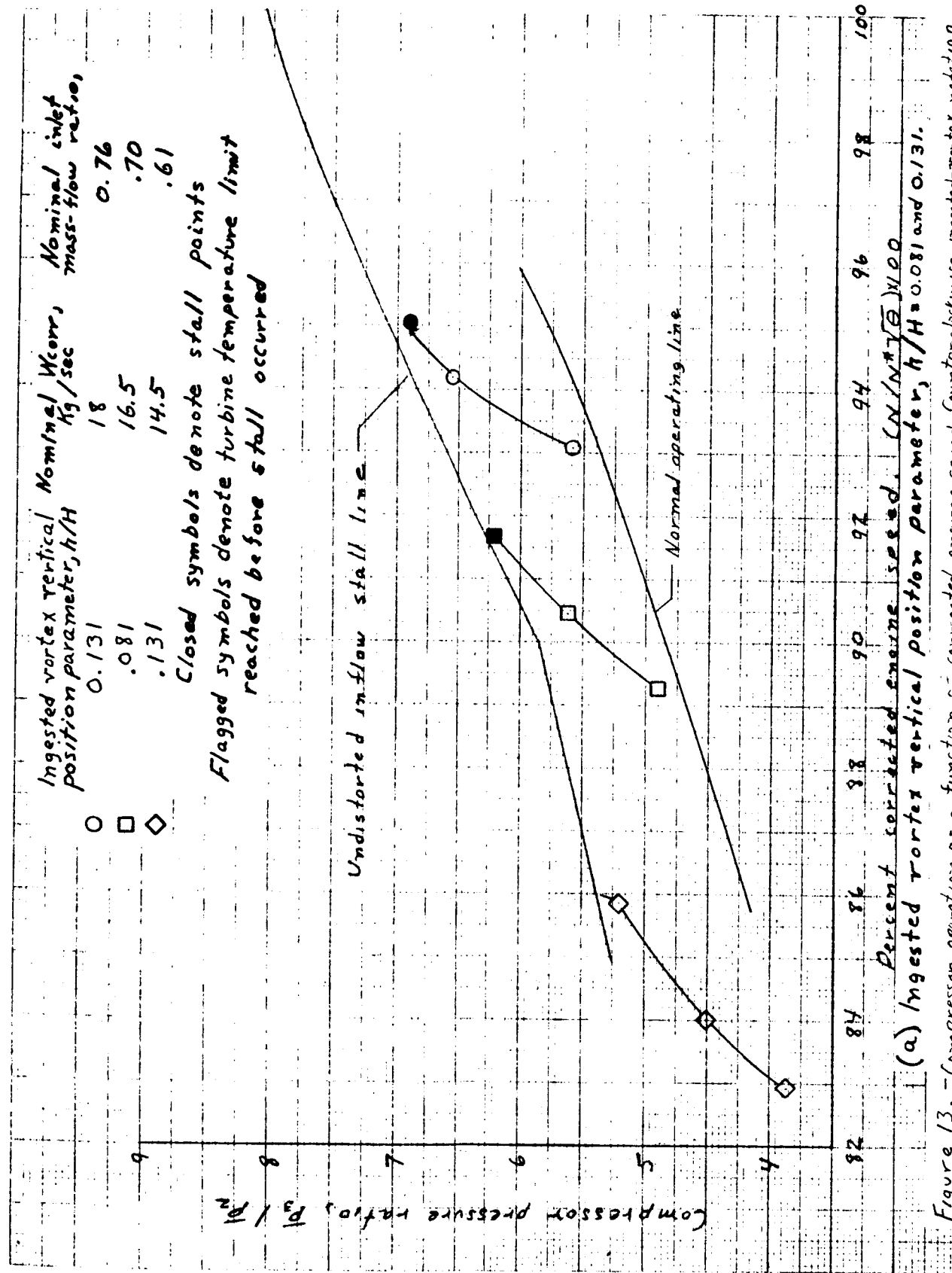
Compressor pressure ratio,  $P_2/P_1$

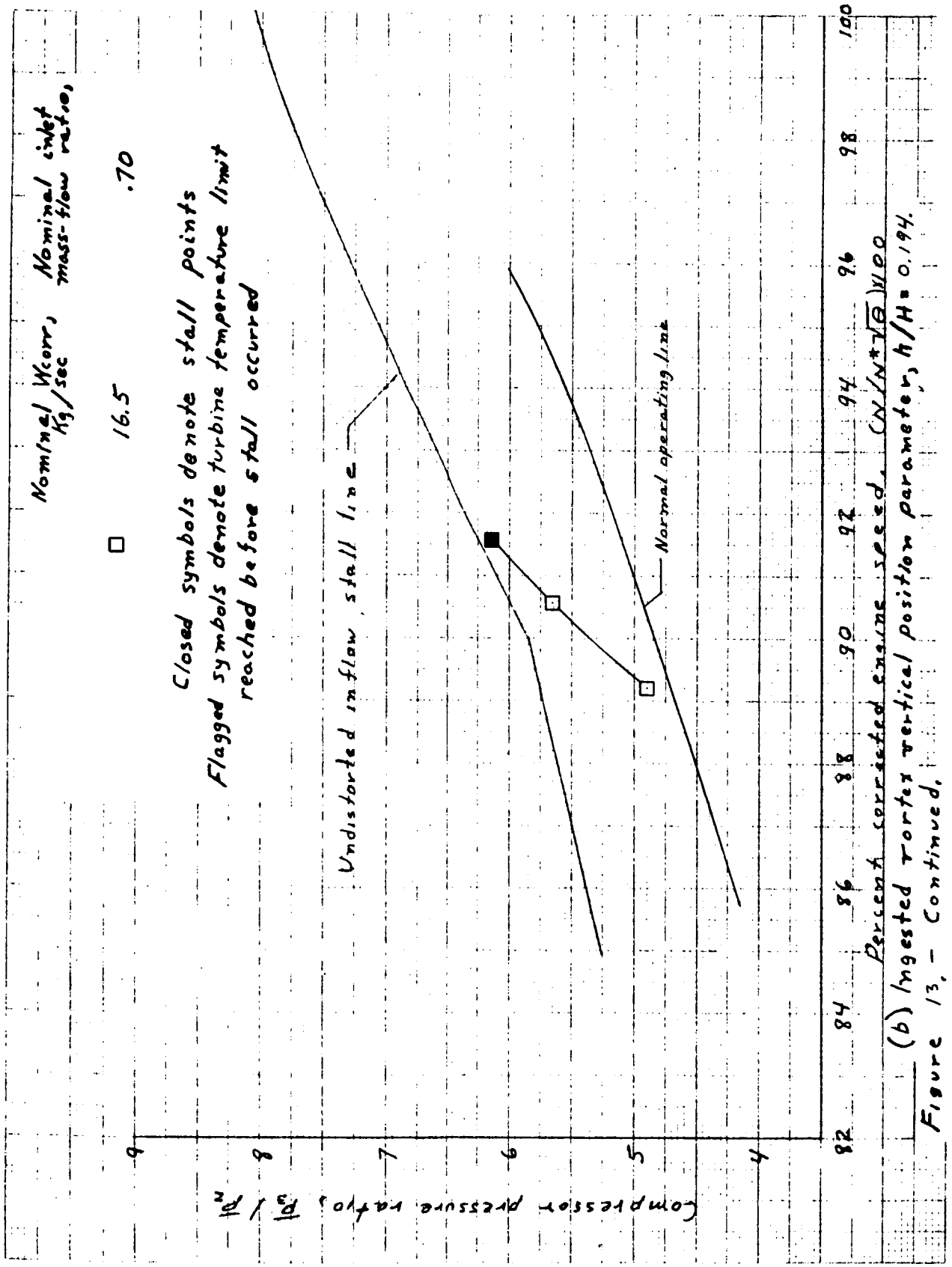
14 15 16 17 18 19 20

Corrected air flow,  $W_{corr}$ ,  $kg/sec$

(h) Ingested vortex vertical position parameter,  $h/H$  0.819 and 0.869.

Figure 12. - Concluded.





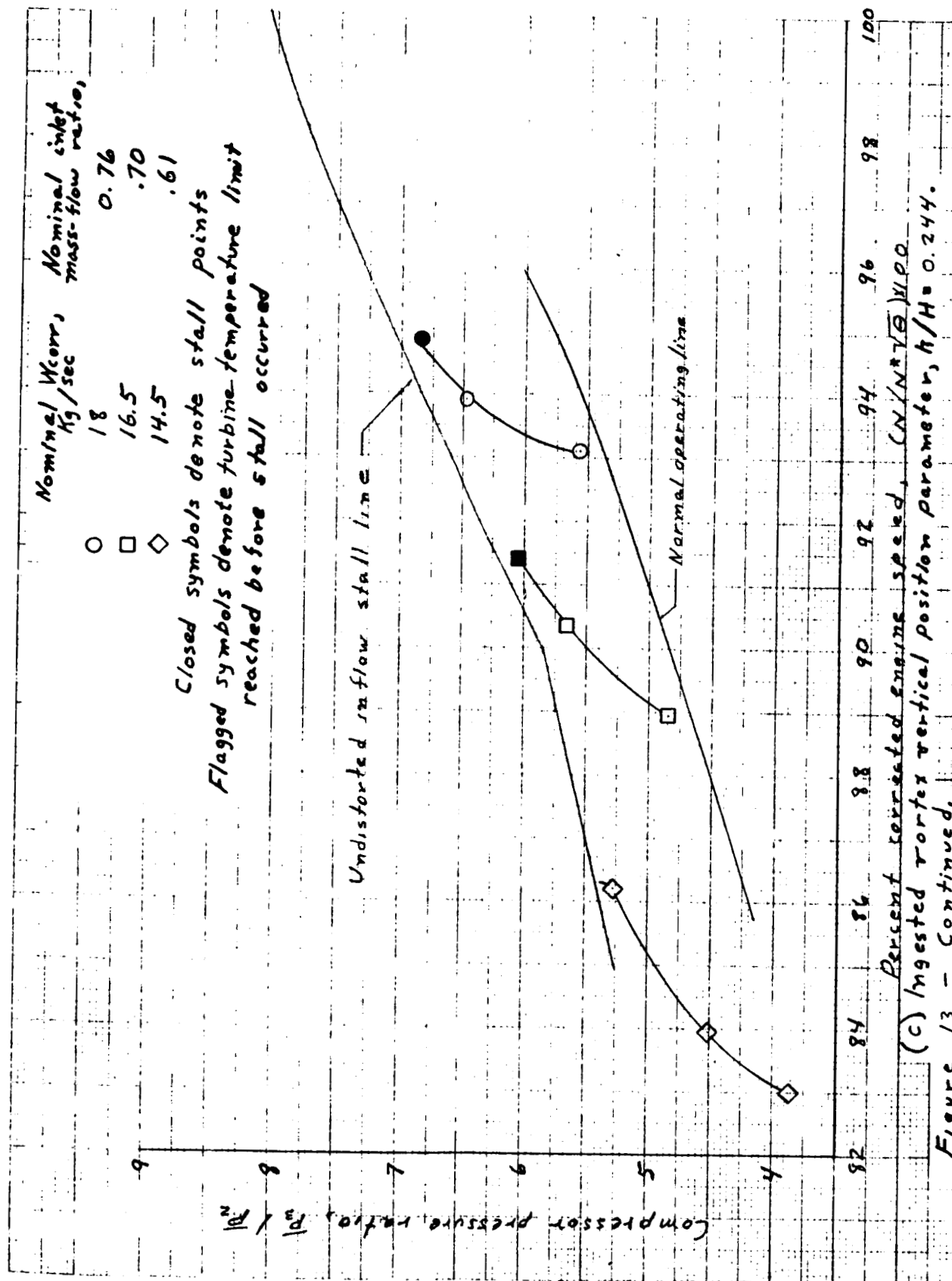
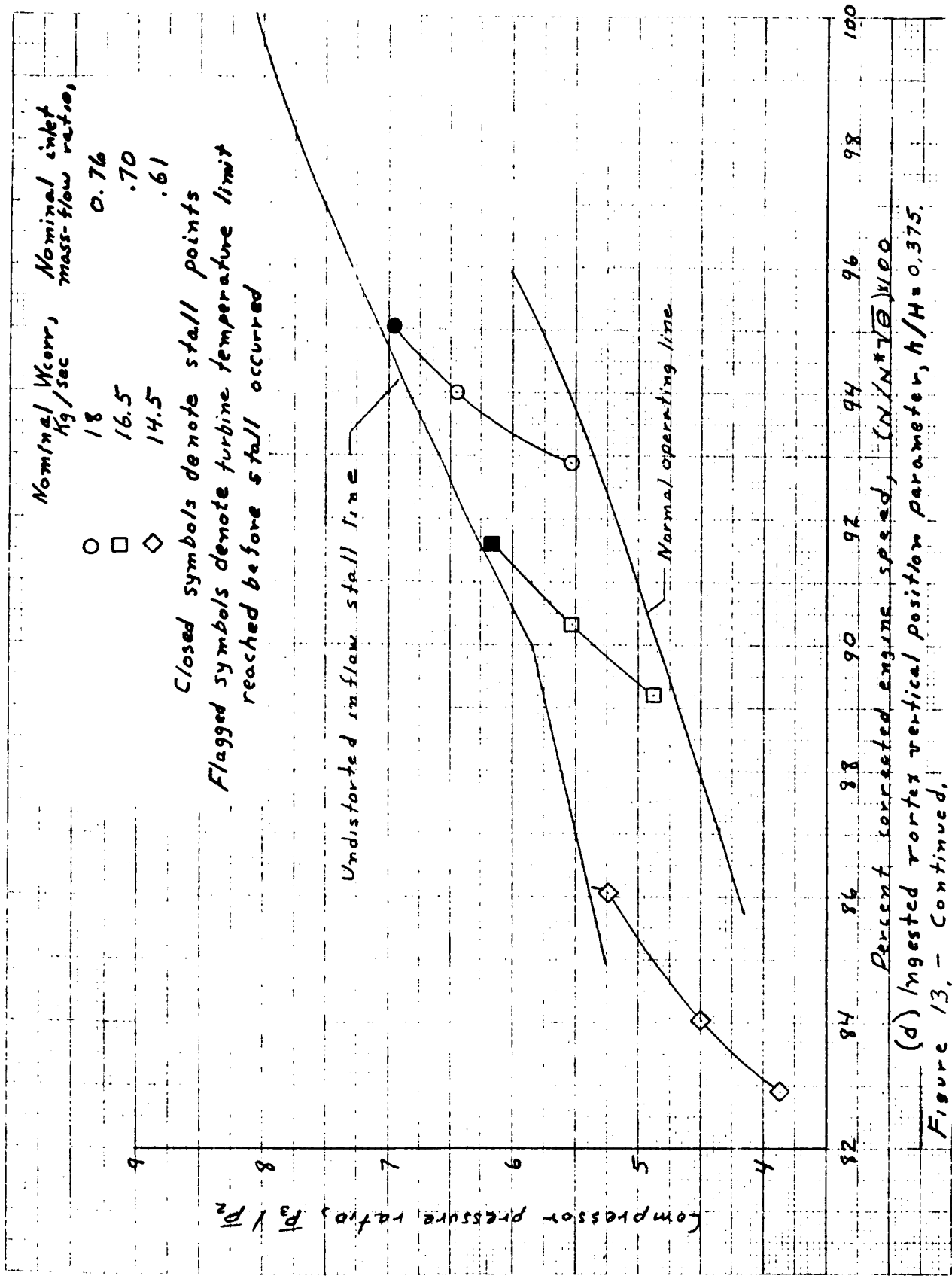


Figure 13. - Continued.

REPRODUCIBILITY OF THE ORIGINAL PAGE IS POOR



(d) Ingested vortex vertical position parameter,  $h/H = 0.375$ .  
 Figure 13, - Continued.

Ingested vortex vertical position parameter,  $h/H$

Nominal  $W_{corr}$ ,  $kg/sec$

Nominal inlet mass-flow ratio,

○

□

◇

0.500

.450

.500

18

16.5

14.5

0.76

.70

.61

Closed symbols denote stall points reached before stall occurred

Flagged symbols denote turbine temperature limit

Undistorted inflow stall line

Normal operating line

Compressor pressure ratio,  $P_3/P_2$

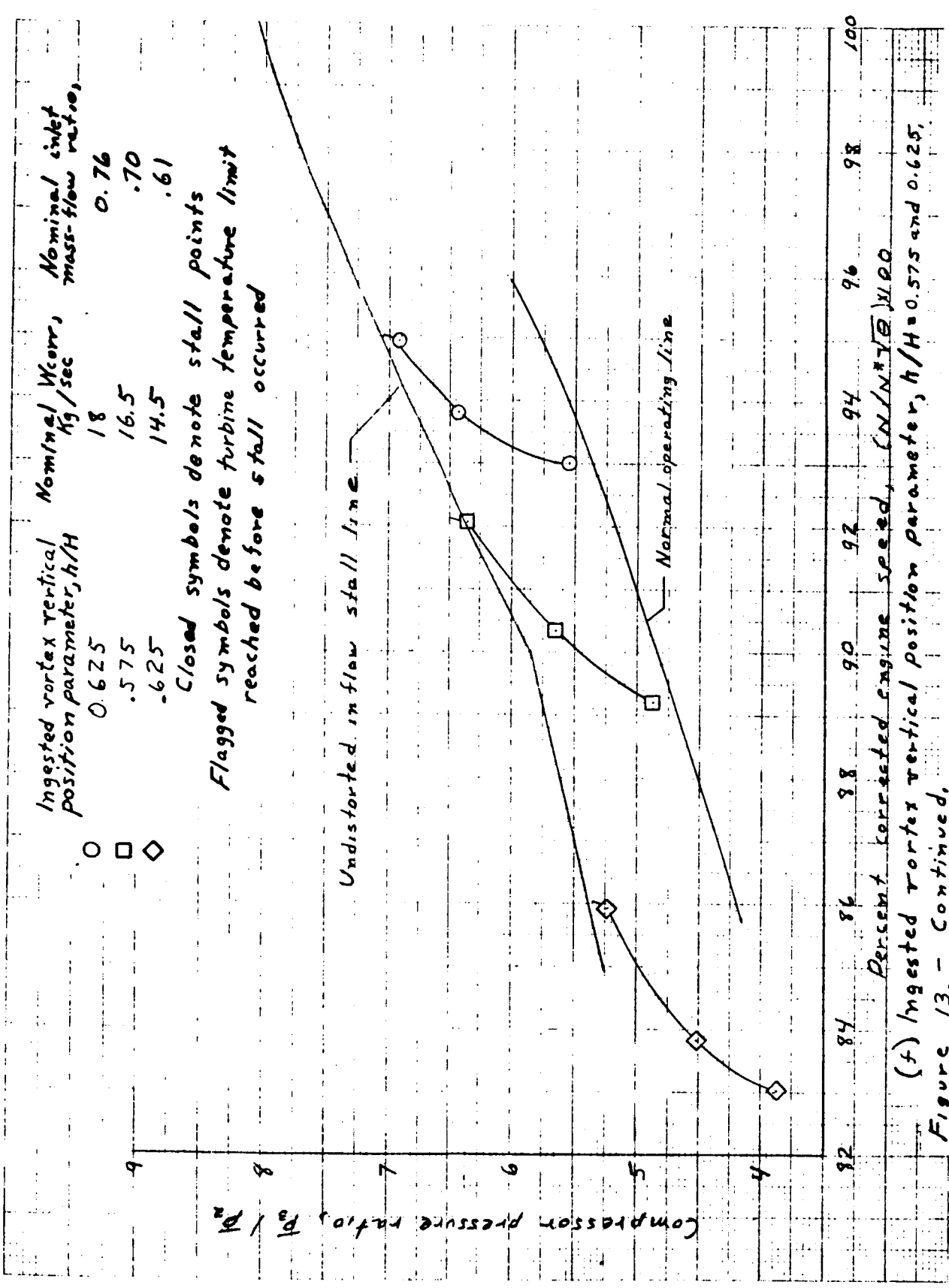
82 84 86 88 90 92 94 96 98 100

Percent corrected engine speed,  $(N/N^*)\sqrt{\theta}/1100$

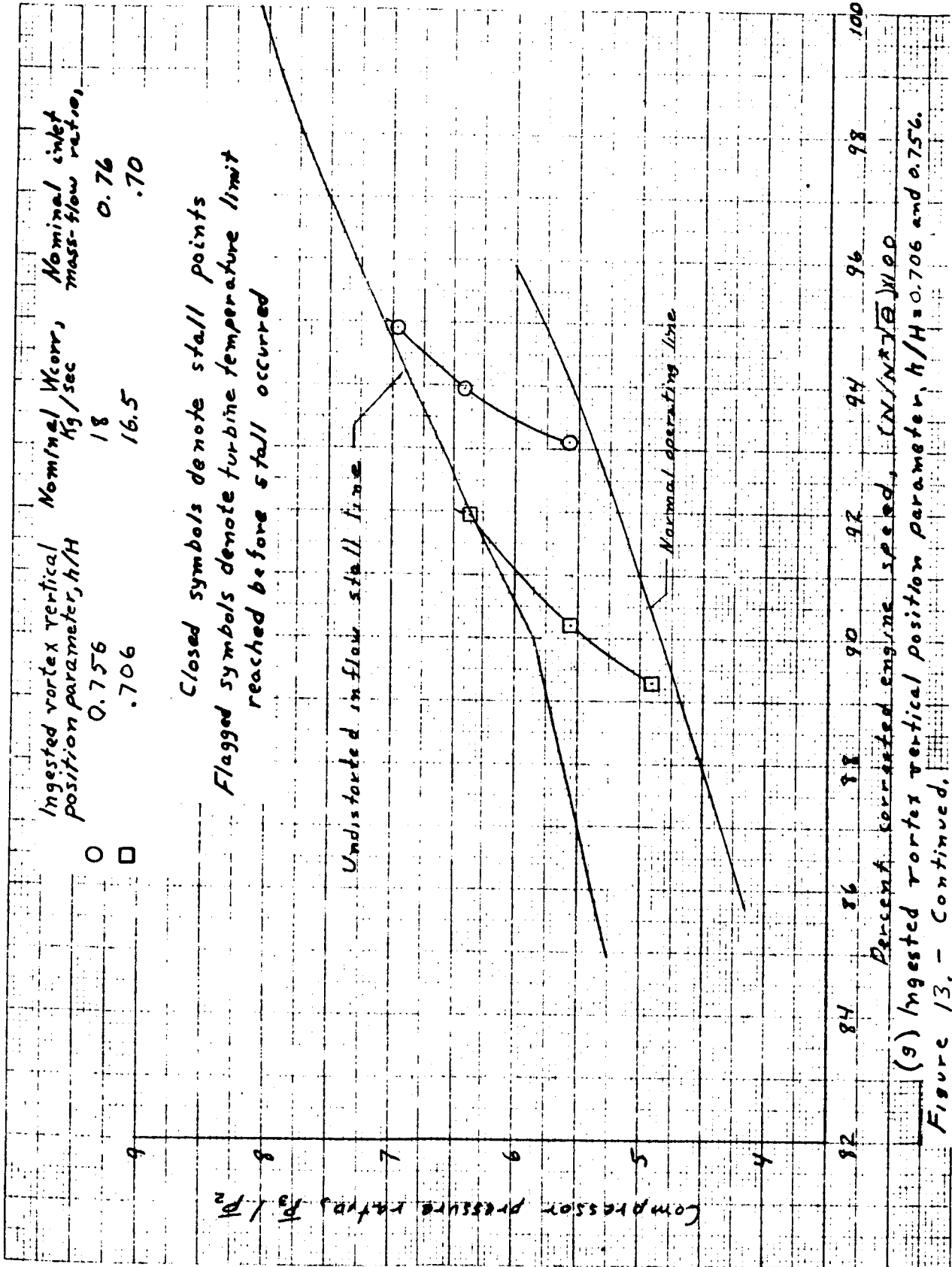
(e) Ingested vortex vertical position parameter,  $h/H = 0.450$  and  $0.500$

Figure 13. - Continued.

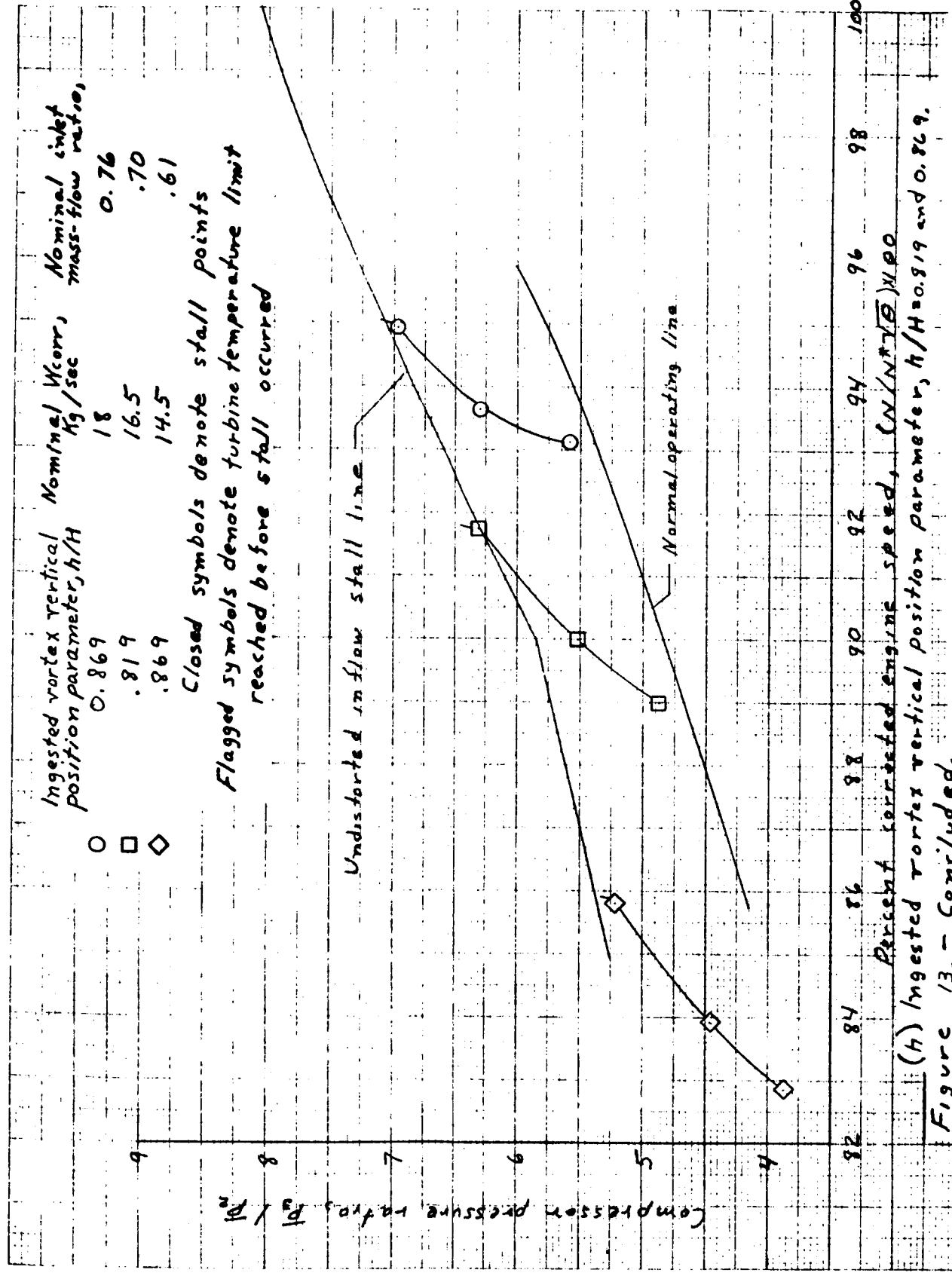
REPRODUCIBILITY OF THE ORIGINAL PAGE IS POOR







REPRODUCIBILITY OF THE  
ORIGINAL PAGE IS POOR



Non-dimensionalized stall compressor pressure ratio at constant corrected speed

$$1 - \left[ \frac{P_2}{P_1} \right]_{stall} / \left( \frac{P_2}{P_1} \right)_a$$

0.02  
0.04  
0.06

0

2

4

6

8

10

12

14

16

18

20

Ingested vortex vertical position parameter,  $h/H$

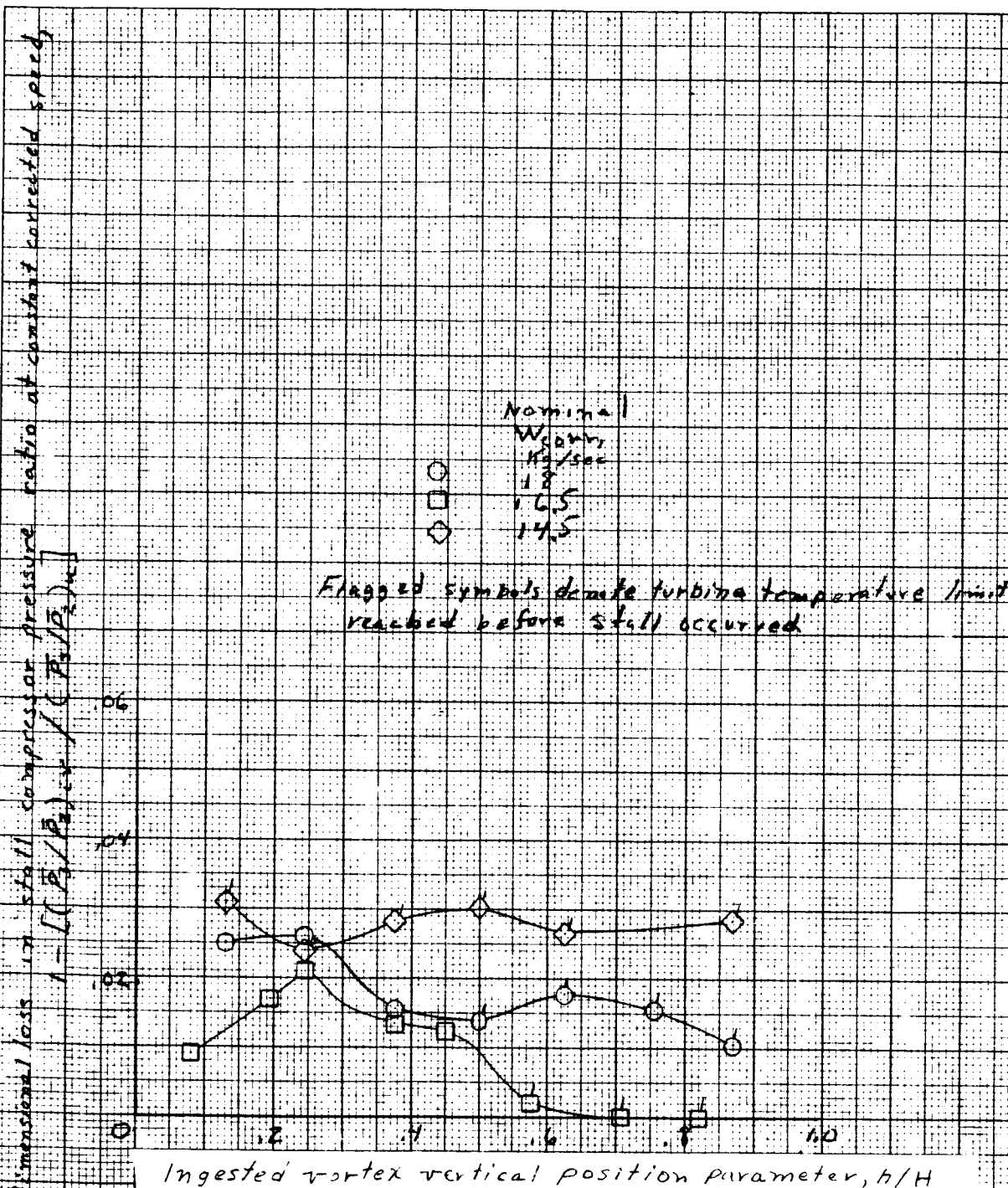
a) Clockwise vortex rotation (counter to engine).

Nominal  
Wt. %  
Kerosene  
18  
16.5  
14.5

Flagged symbols denote turbine temperature limit reached before stall occurred

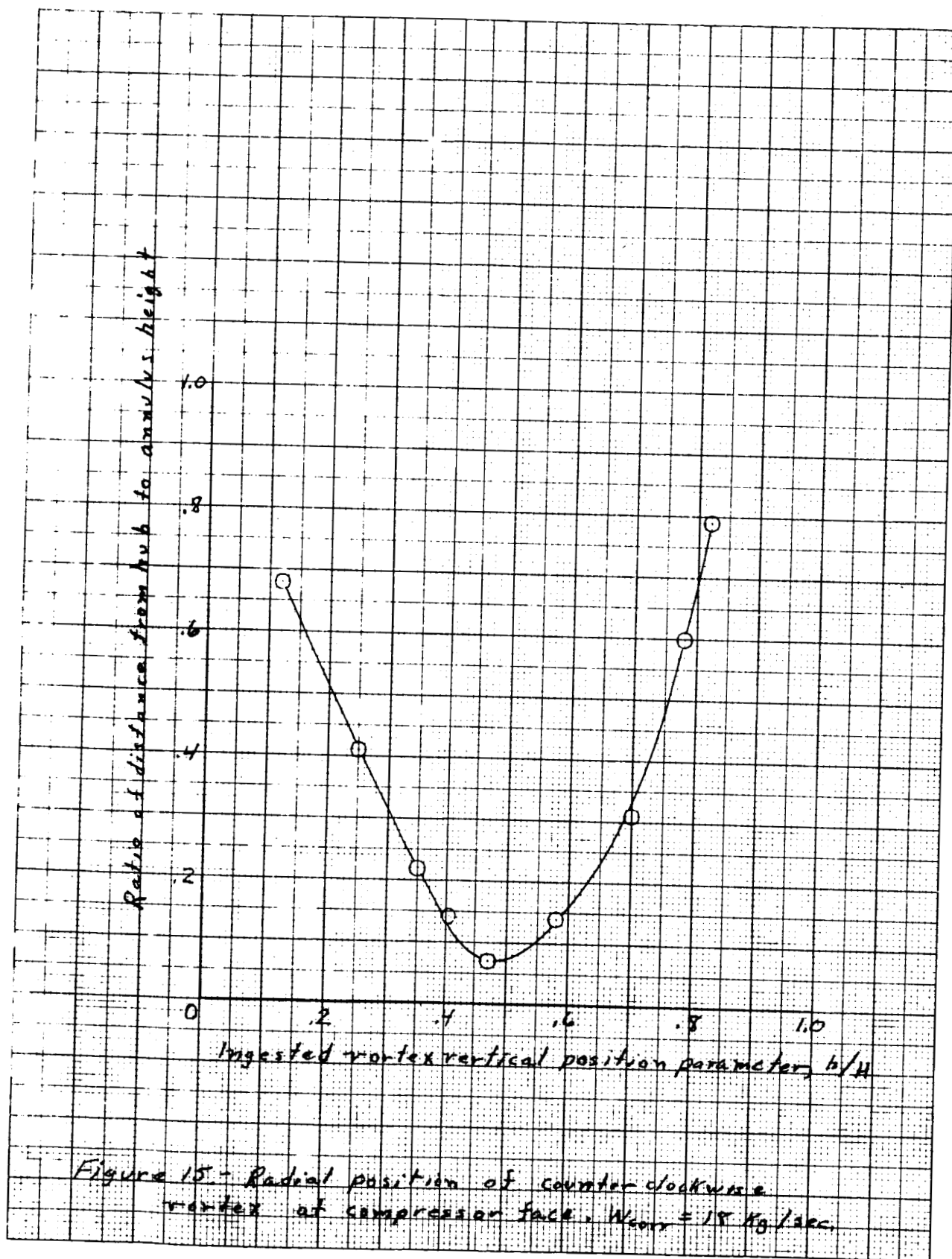
Figure 14.- Effect of vertical placement of ingested vortex on compressor stall.

REPRODUCIBILITY OF THE  
ORIGINAL PAGE IS POOR



b) Counter clockwise vortex rotation (with engine).

Figure 14.- Concluded.



NASA Lewis-Coml., Cleve., OH.

REPRODUCIBILITY OF THE  
ORIGINAL PAGE IS POOR